Numerical Simulations of the Fourth Avenue Landslide Considering Cyclic Softening

by

Michael J. Kiernan

A thesis submitted to the Graduate Faculty of
Auburn University
in partial fulfillment of the
requirements for the Degree of
Master of Science

Auburn, Alabama
May 4, 2019

Keywords: deformation analyses, sensitive clay, strain softening, numerical analysis

Approved by

Jack Montgomery, Chair, Assistant Professor of Civil Engineering
J. Brian Anderson, Associate Professor of Civil Engineering
Marta Miletic, Assistant Professor of Civil Engineering

ABSTRACT

Cyclic softening of fine grained soils has led to significant infrastructure damage in previous earthquakes. Despite this, methods to evaluate the potential deformations due to cyclic softening are not as well developed as methods to evaluate potential deformations due to earthquake induced liquefaction. This is especially true for numerical analyses where clayey soils are often modeled using a single undrained strength without considering the potential for strength loss. When strain softening is considered, the solution may become mesh dependent leading to unreliable results. This paper explores the use of two separate constitutive models to model the cyclic softening behavior of a mildly sensitive clay. The first constitutive model studied is a total stress based strain softening model with a softening-scaling based regularized implemented to provide an approximately mesh insensitive solution. The second constitutive model investigated is a critical state compatible effective-stress model which has been modified to model structural degradation of a sensitive soil. The Fourth Avenue landslide, which was initiated by the 1964 Great Alaska Earthquake, is used for this numerical evaluation. Deformation patterns and magnitudes from numerical simulations are compared to site observations. Uncertainty due to the choice of the input ground motion and the material properties are explored along with the effects of changing the density of the mesh. Practical implications of each model are discussed as well as potential limitations.

ACKNOWLEDGEMENTS

I would first like to thank my advisor and committee chair Dr. Jack Montgomery. I could not have asked for a better mentor. Thank you for taking a chance on me. I would also like to acknowledge the other committee members, Dr. J. Brian Anderson and Dr. Marta Miletic. Their lessons and guidance over the past few years have been invaluable. I would like to recognize the authors of the PM4Silt and PM4Sand constitutive models, Dr. Ross Boulanger and Dr. Katerina Ziotopoulou. Your contributions have not only advanced the field of geotechnical modeling but have provided research opportunities for students like me. I would also like to thank my parents, Dennis and Wendy Bowers. I could have never gone back to college without their unwavering support. Most importantly I need to thank my wife, Lindsey Kiernan. She has sacrificed a great deal so that I can pursue my ambitions. You have been selfless, and I could not be more grateful.

TABLE OF CONTENTS

LIST OF TABLES

LIST OF FIGURES

LIST OF ABBREVIATIONS AND SYMBOLS

a	K_f line intercept in p-q space
c	Mohr-Coulomb cohesion intercept
BCC	Bootlegger Cove Clay
CPT	Cone Penetration Test
CRR	Cyclic Resistance Ratio
CSR	Cyclic Stress Ratio
CVRS	Constant Volume Ring Shear
DLL	Dynamic Link Library in FLAC
D_R	Relative Density
DS	Direct Shear Test
DSS	Direct Simple Shear Test
γ_{elem}	Shear Strain at Element Level
γ_{rem}	Remolding Strain
γ_{sb}	Shear Strain at Shear Band Level
g	Gravity Units
G_o	Shear Modulus Coefficient in PM4Silt and PM4Sand
h_{elem}	Height of Element
h_{sb}	Height of Shear Band (Shear Band Thickness)

h_{po}	Contraction Rate Parameter in PM4Silt and PM4Sand
h_o	PM4Silt/ PM4Sand Variable That Adjusts Ratio of Plastic to Elastic Modulus
K_f	Mohr-Coulomb failure envelope in p-q space
m	Meters
$(N_1)_{60}$	Energy and Overburden Corrected SPT Blow Count
$n^{b,wet}$	PM4Silt parameter that Controls the Peak Undrained Shear Strength
NDAs	Non-Linear Deformation Analyses
N_{kt}	CPT Cone Factor
OCR	Overconsolidation Ratio
p	Mean stress
PGA	Peak Ground Acceleration
PI	Plasticity Index
Ψ	Slope of K_f line in p-q space
q	deviator stress
Γ	Critical State Line Intercept at 1 kPa
$\Gamma_{initial}$	Initial Critical State Line Intercept at 1 kPa
$\Gamma_{residual}$	Residual Critical State Line Intercept at 1 kPa
SPT	Standard Penetration Test
S_t	Sensitivity
$\frac{S_{u,res}}{\sigma'_v}$	Residual Undrained Shear Strength Ratio
$\frac{S_{u,cs,eq}}{\sigma'_v}$	Undrained Shear Strength Ratio at Critical State Under Seismic Loading in PM4Silt
$\frac{S_{u,pk}}{\sigma'_v}$	Peak Undrained Strength Ratio

CHAPTER 1: INTRODUCTION

1.1 Background

The potential for strength loss in fine grained soils poses a significant hazard for many geotechnical projects. Damage to infrastructure attributed to strain softening of clayey soils has been documented in many case histories involving both static (e.g., Gregersen 1981, Locat et al. 2017) and cyclic loading (e.g., Shannon and Wilson 1964, Heritage 2013, Nakamura et al. 2014). For critical infrastructure projects, potential deformations due to cyclic loading are increasingly being analyzed using nonlinear deformation analyses (NDAs). These analyses rely on constitutive models which can represent the aspects of soil behavior important to the problem being analyzed. Multiple validated constitutive models are available to evaluate potential deformations due to liquefaction of granular soils (e.g., Elgamal et al. 2002, Beaty and Byrne 2011, Boulanger and Ziotopoulou 2017), but relatively few models are available to evaluate potential deformations due to cyclic softening in clayey soils.

Simple total stress based models exist which have many practical applications but do not accurately capture all important aspects of soil behavior (e.g., Anderson and Jostad 2005, Beaty and Dickenson 2015). These models often implement a simplified representation of stress-strain response fitted to empirical data and cannot account for coupling between the soil and pore fluid (Taibet et al. 2011). Complex effective stress based models that can treat the soil and pore fluid separately present another option (e.g., Park 2011, Seidalinov and Taibet 2014, Boulanger and Ziotopoulou 2018). Effective stress models are often grounded in a comprehensive theoretical framework and tend to better capture nonlinear dynamic soil response (Lim et al. 2010). They may however require tedious calibration involving numerous input parameters which may not be directly available from standard lab tests (Hsieh et al. 2010).

Strain localization presents an additional challenge when modeling cyclic softening of clays. In clays, strains tend to localize into thin shear bands during softening which can accelerate strength loss (Park 2011). The residual soil strength where the shear band initiated may be reached before residual strength along the complete failure surface is mobilized (Park 2011). The stress required to activate a landslide may consequently be achieved prior to full softening of the material along the entire shear surface (Figure 1). Natural shear banding has been observed in lab tests and in the field. Henkel and Skempton (1955) described a distinct shear plane through a clay layer in the Jackfield landslide, though the thickness of the localized region was not reported. Park (2011) observed localized shear zones in centrifuge tests involving dynamic loading of weakly cemented sensitive clay slopes. Gylland et al. (2014) presents a clear example of shear banding in a sensitive clay specimen sheared in a triaxial test. (Figure 2).

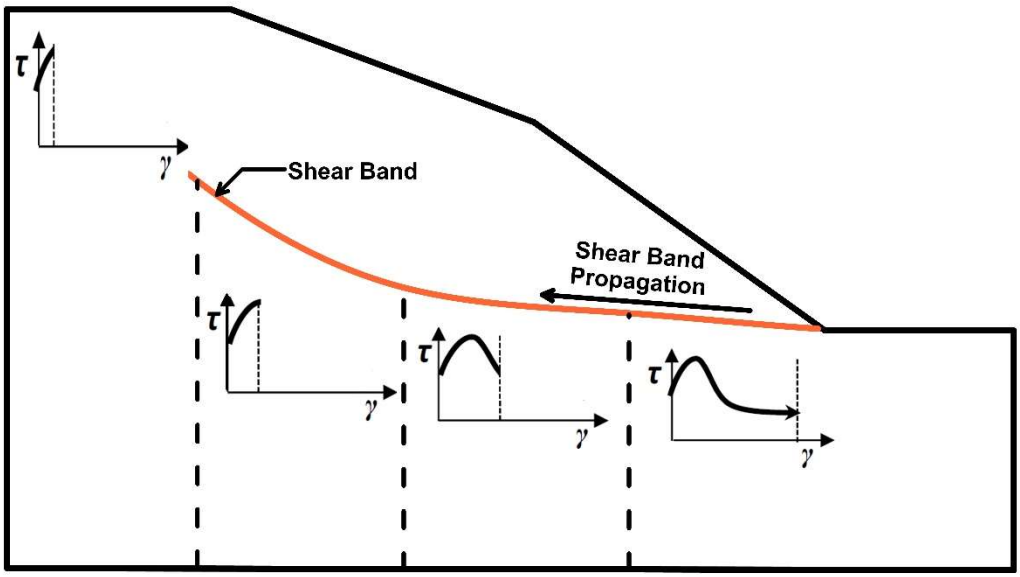

Figure 1: Example states of stress and strain along different regions of propagating shear band (after Park 2011)

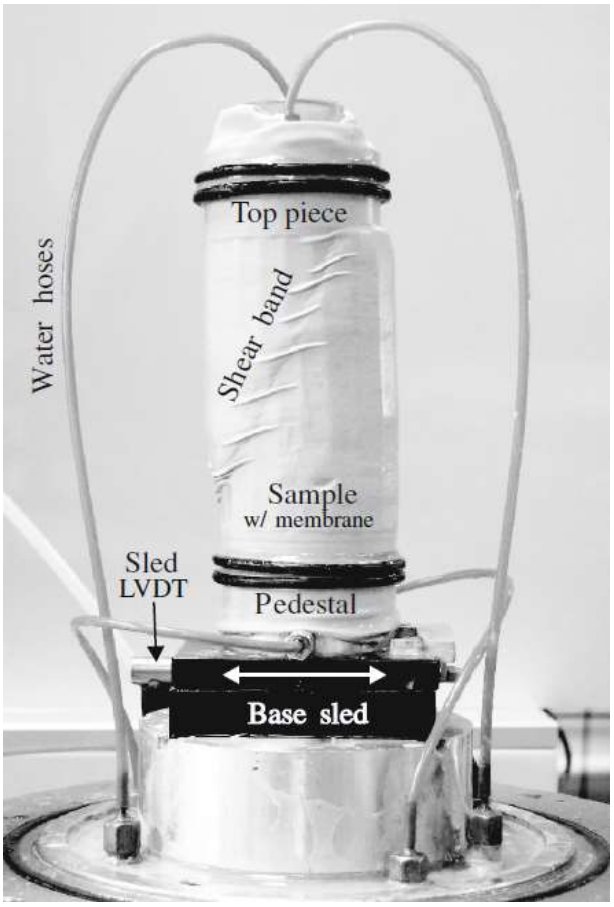

Figure 2: Example of shear band observed in triaxial test (from Gylland et al. 2014)

In numerical simulations, strains tend to localize over a single row of elements resulting in a mesh dependent solution (Thakur et al. 2006). The major challenge in modeling strain softening is how to define the shear band numerically once localization initiates. To overcome this, various approaches have been developed and applied to clays including softening-scaling (e.g., Pietruszczak and Mróz 1981), non-local constitutive models (e.g., Brinkgreve 1994), interface elements (e.g., Jostad and Andersen 2004), extended finite elements (e.g., Septanika et al. 2007), rate dependent models (e.g., Park 2011) and pore fluid coupling (e.g., Thakur et al. 2005). Such methods which are used to address mesh dependency of numerical solutions are generally referred to as regularization techniques.

The term sensitivity is used in two separate contexts in this document. The difference between these two definitions of sensitivity is described here to avoid confusion. The first definition will be referred to as clay sensitivity, or Bootlegger Cove Clay (BCC) sensitivity, which describes the amount of strength loss expected for a sensitive strain softening clay. Clay sensitivity (S_t) is defined as the ratio of the peak undrained shear strength to the residual undrained shear strength of the clay. The term numerical sensitivity will also be used in this document. Numerical sensitivity describes how the numerical solution responds to variations in model parameters such as material calibrations, input ground motions or mesh size.

1.2 Objective and Scope

The objective of this study is to evaluate the ability of two different constitutive models to accurately reproduce earthquake induced deformation patterns and magnitudes resulting from strain softening of a mildly sensitive clay. The first constitutive model studied is a Mohr-Coulomb based total stress model which can represent strain softening by allowing the undrained shear strength to decrease with increasing plastic shear strain. A softening-scaling based regularization technique is also implemented into the total stress model in an attempt to reduce mesh dependency of the solution. This proposed constitutive model will be referred to as the regularized strain softening model.

The second constitutive model studied is a modified version of PM4Silt (Boulanger and Ziotopoulou 2018). PM4Silt is an effective stress based critical state compatible bounding surface plasticity model which is formulated to represent the cyclic behavior of low plasticity fine grained soils. The PM4Silt model requires few input parameters from the user with a relatively straightforward calibration procedure. PM4Silt is modified by the author such that the critical state line intercept at 1 kPa decreases with increasing plastic shear strain to model structural degradation

inherent to sensitive clays. This proposed constitutive model will be referred to as the modified PM4Silt model.

The case history chosen for evaluation is the Fourth Avenue Landslide which occurred during the 1964 Great Alaska Earthquake. Simulation results from finite difference analyses are compared to observed deformations at the Fourth Avenue site using each model. Limited numerical sensitivity studies are performed for each model to examine how variations in input motion and model parameters affect the results. Mesh dependency of the solutions are also investigated. Practical implications of the results from each p model are discussed as well as potential limitations.

1.3 Organization of Thesis

Chapter 2 provides background information regarding the chosen case history. The Great Alaska earthquake and resulting ground failures in the Anchorage area are presented first. The Fourth Avenue slide that was chosen for numerical evaluation is then described in detail using information published by Shannon and Wilson (1964). Site investigations performed near the Fourth Avenue site by previous researchers (Shannon and Wilson 1964, Woodward-Clyde 1982, Nath et al. 1997, Stark and Contreras 1998) are used to determine general soil properties for each soil layer and compared to values selected by Beaty and Dickenson (2015). The ground motions used in this study are finally presented and discussed.

Chapter 3 is focused on numerical simulations using the regularized strain softening Mohr-Coulomb model. The selected constitutive model and regularization technique are discussed as well as similar regularization techniques, which have been successfully implemented by previous authors (e.g., Pietruszczak and Mróz 1981, Potts et al. 1990, Anastasopoulos et al. 2007). The modeling approach used in this chapter is then discussed in regard to constitutive models, boundary

conditions, model initialization and application of the input motions. Input parameters used for the BCC with the regularized strain softening model are then discussed. Simulation results are finally presented and examined. The information in this chapter is based on research previously published by Kiernan and Montgomery (2018) but slight changes have been made so that the soil properties used are more consistent with the values used in Chapter 4 of this paper.

Chapter 4 is focused on numerical simulations using the modified PM4Silt constitutive model. The modeling approach used in this chapter is first presented in terms of boundary conditions, model initialization and application of the input motions. Constitutive models for dynamic loading are then addressed as well as the required calibration procedures. The modification of the PM4Silt model used for the critical BCC layer is then outlined as well as the calibration procedure. Simulation results are finally presented and discussed. The information in this chapter has been previously published by Kiernan and Montgomery (2019).

Chapter 5 summarizes the results of this study and draws conclusions based on the modeling results and discussions. Practical implementations for each model are discussed as well as potential limitations.

CHAPTER 2: CASE HISTORY AND BACKROUND INFORMATION

2.1 Great Alaska Earthquake

The Fourth Avenue landslide was initiated by the 1964 Great Alaska Earthquake on March 27th, 1964. The moment magnitude (Mw) 9.2 earthquake was caused by the rupture of a subduction zone interface near Prince William Sound (Ichinose et al. 2007). Ground motions recordings for this event do not exist, but eyewitness accounts and damage patterns estimate two to three minutes of strong shaking and a PGA of up to 0.2 g (Moriwaki 1985). Ground failures were extensive in the Anchorage area; approximately 120 km from the epicenter of the earthquake. Figure 3 shows the relative locations and slide mass areas for some notable landslides induced by the ground shaking including the Turnagain, L Street, Government Hill, and Fourth Avenue landslides. Figure 4 shows the damage caused by each of these landslides. Cyclic softening of the sensitive Bootlegger Cove Clay (BCC) presents a common link between each of these failures (Shannon and Wilson 1964).

2.2 Fourth Avenue Landslide

Cyclic softening of the strain softening BCC layer due to ground shaking is the likely cause of the Fourth Avenue landslide. The Fourth Avenue slide mass was 490 m long and 275 m wide with maximum lateral displacements over 5m near the bluff at Fourth Avenue (Idriss 1985). Graben formation was observed on the bluff behind the slide mass and pressure ridges were observed near the toe of the slope (Shannon and Wilson 1964). Eyewitness accounts suggest the slide initiated about 2 minutes after the shaking began with slide movement ceasing about the same time ground shaking stopped (Hanson 1965).

The Fourth Avenue landslide was chosen for numerical evaluation in this study due to its simple stratigraphy and failure mechanism as well as the extensive site characterizations

performed in the area. A simplified cross-section of the Fourth Avenue slide with observed deformations is shown in Figure 5 as estimated from investigations performed by Shannon and Wilson (1964). Figure 6 shows the ground deformation patterns observed at the Fourth Avenue site as presented by Shannon and Wilson (1964) with the location of the selected cross section represented by the blue line for reference. The boring locations used to estimate the cross section are also shown by orange squares on Figure 6 and are documented in Shannon and Wilson (1964). The simplified cross section in Figure 5 is comparable to those presented by previous researchers (e.g., Shannon and Wilson 1964, Idriss 1985, Stark and Contreras 1998, Beaty and Dickenson 2015).

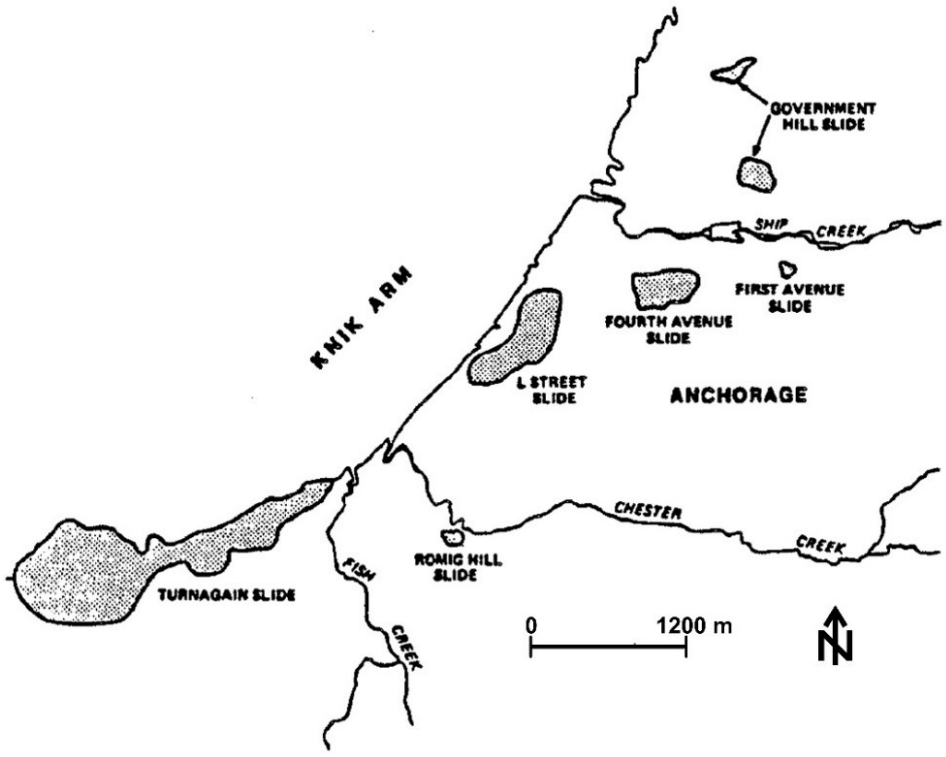

Figure 3: Relative locations and sizes of notable ground failures caused by the Great Alaska Earthquake. Figure taken from Moriwaki et al. (1985) with scale and North arrow added by author.

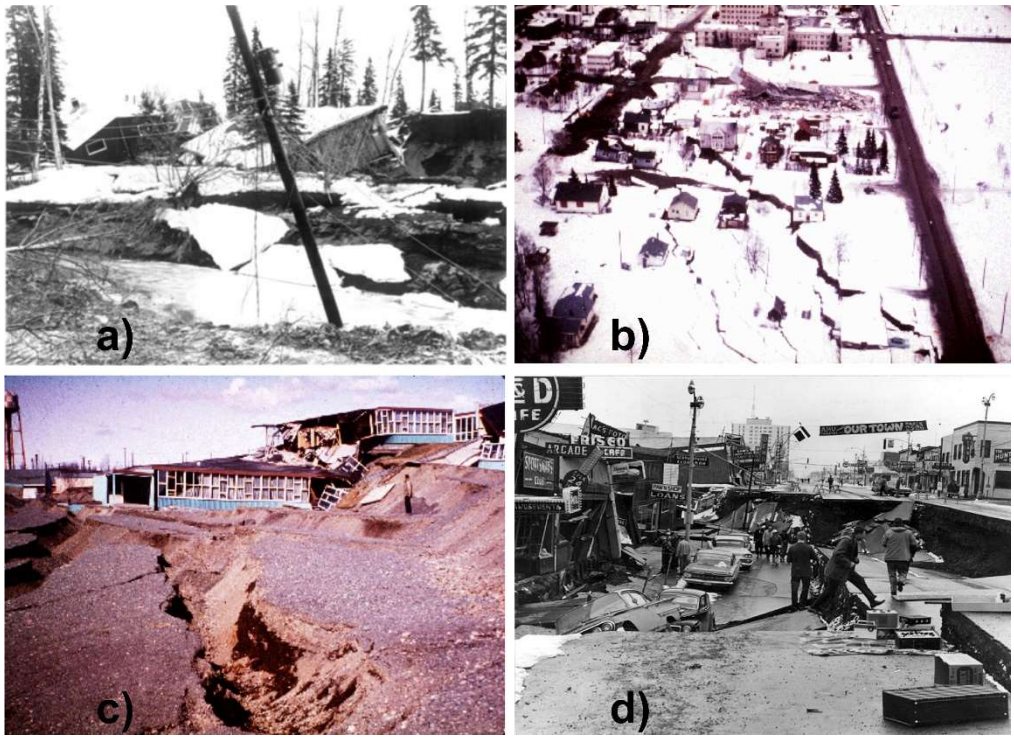

Figure 4: Damage at (a) Turnagain landslide; (b) L Street landslide; (c) Government Hill landslide; (d) Fourth Avenue landslide. Photos from earthquake.usgs.gov/earthquakes/events/alaska1964/1964pics.php

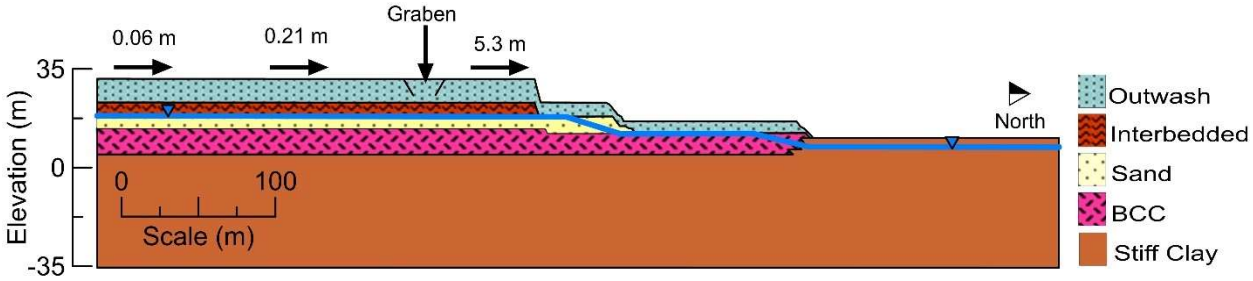

Figure 5: Cross-section of the Fourth Avenue landslide with observed deformations (after Shannon and Wilson 1964)

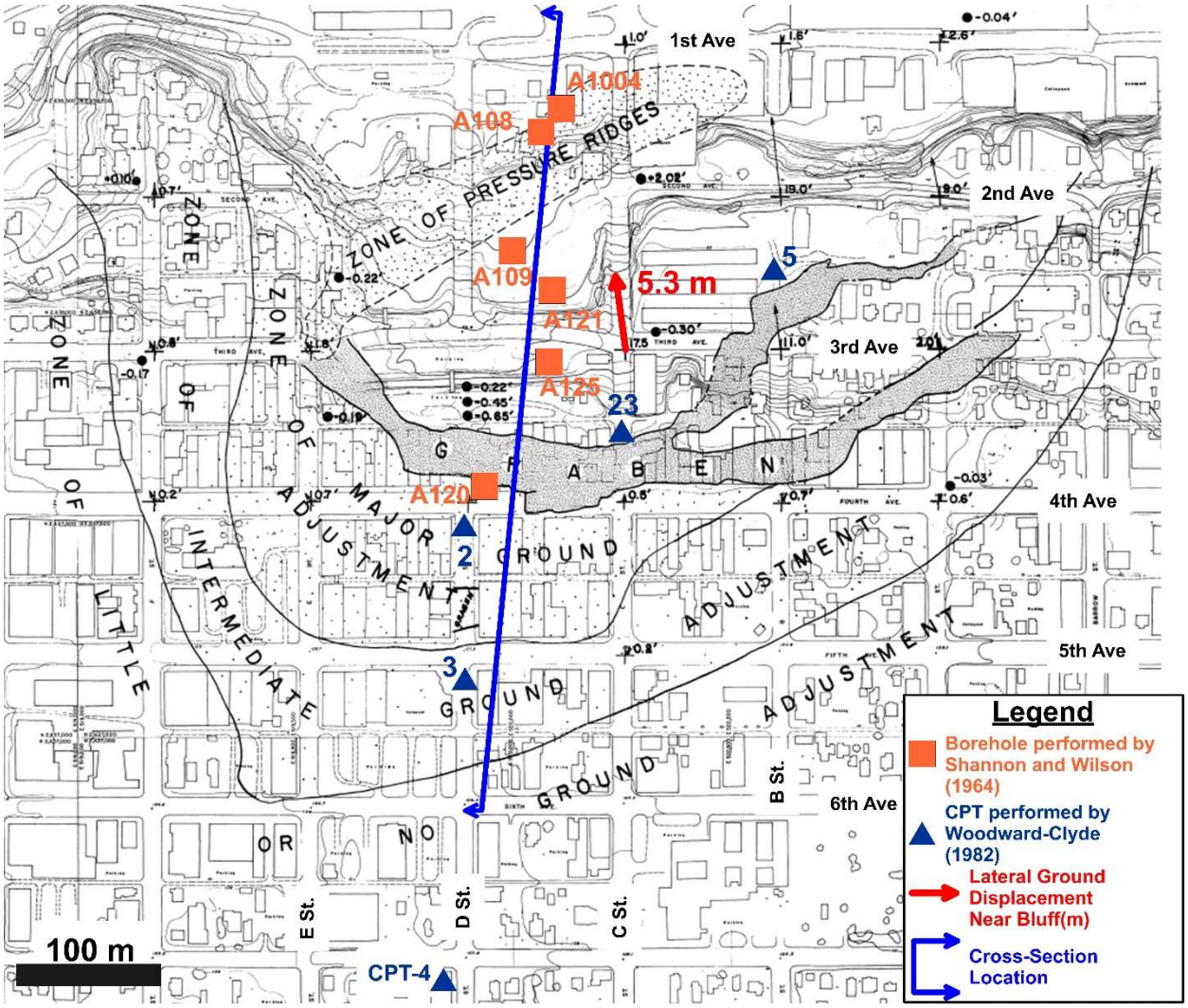

Figure 6: Fourth Avenue landslide ground displacements (from Shannon and Wilson 1964) with locations of chosen cross section, borings (performed by Shannon and Wilson 1964) and CPTs (performed by Woodward-Clyde 1982)

2.3 Site Investigations and General Soil Properties

Site investigations for the Fourth Avenue site consist of standard penetration tests (SPTs), field vane tests and index tests performed by Shannon and Wilson (1964). Woodward-Clyde (1982) performed SPTs, CPTs, miniature vane shear tests, direct simple shear (DSS) and direct shear (DS) tests. Constant volume ring shear tests (CVRS) were also performed on BCC specimens

by Stark and Contreras (1998). The locations of the CPTs by Woodward-Clyde (1982) used in this study are represented by dark blue triangles in Figure 6. Shear wave velocities were estimated using results from downhole tests at a nearby site (Nath et al. 1997). The selected shear wave velocity profile from this study (Figure 7) is consistent with those of previous researchers (e.g., Beaty and Dickenson 2015). The general soil properties selected for each soil layer are shown in Table 1 and are consistent with those chosen by Beaty and Dickenson (2015). Specific soil properties and input parameter values used for dynamic loading with each proposed constitutive model are discussed in detail in the follow chapters.

Table 1: Estimated soil properties for each layer

	Outwash	Interbedded	Sand	BCC	Stiff Clay
γ_{moist} (kN/m^3)	20.0	19.5	19.5	18.5	20.0
ϕ' (deg)	38	35	35	30	35
v_s (m/s)	300	300	300	220	450
S_u/σ'_v	N/A	0.35	N/A	0.23	0.35

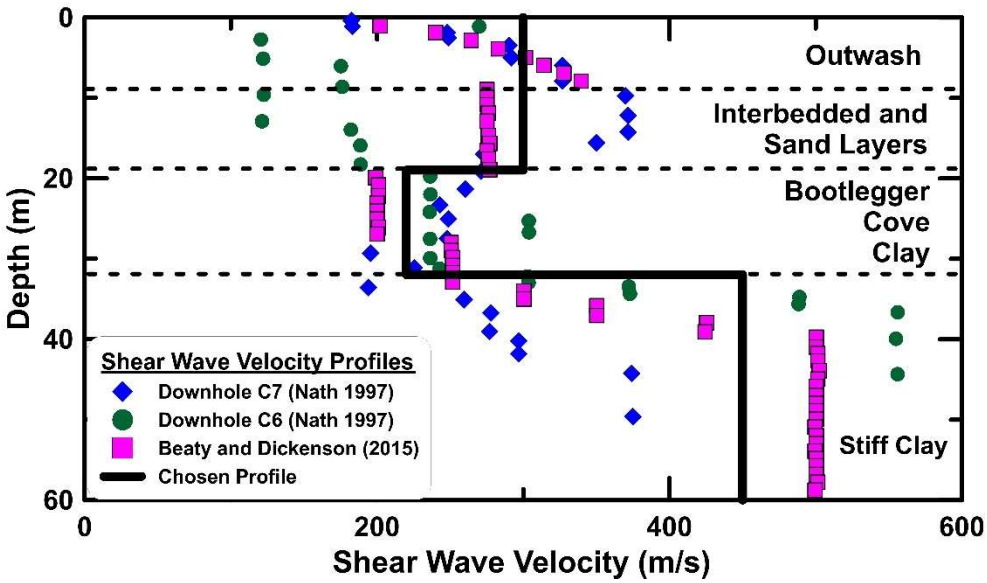

Figure 7: Shear wave velocity profile for Fourth Avenue site

2.3.1 BCC General Soil Properties

The sensitive BCC typically classifies as a low plasticity silty clay with PI values below 20 and LL values around 35 (Shannon and Wilson 1964, Moriwaki et al. 1985). The peak undrained shear strength ratio ($S_{u,pk}/\sigma'_v$) for the critical BCC layer was calculated from equation 1 provided by Woodward-Clyde (1982) which was derived from DSS tests (Figure 8). Woodward-Clyde (1982) reported a mean OCR of 1.3 for the BCC. Using equation 1 with an OCR of 1.3 the value of $S_{u,pk}/\sigma'_v$ for the BCC used in this study was calculated to be 0.23. It should be noted that this value is on the low end of the range of undrained shear strength ratios reported by Stark and Contreras (1998) which ranged from 0.23 to 0.28 based on CVRS tests. DSS tests are thought to better represent seismic loading conditions and are therefore considered most appropriate for selecting the undrained shear strength ratios for this study.

$$\frac{S_{u,pk}}{\sigma'_v} = 0.185(OCR)^{0.78} \quad (1)$$

The term clay sensitivity (S_t) describes the amount of strength loss expected for a strain softening material and is defined as the ratio of peak undrained shear strength to remolded undrained shear strength. Idriss (1985) reported BCC sensitivities ranging from 2 to 11 with an average clay sensitivity of 3.3 based on miniature vane shear tests, CPTs, and DS tests. Stark and Contreras (1998) report a clay sensitivity near 4 for the BCC in the slide area based on CVRS tests. The shear wave velocity of the BCC was estimated to be 220 m/s (Figure 7).

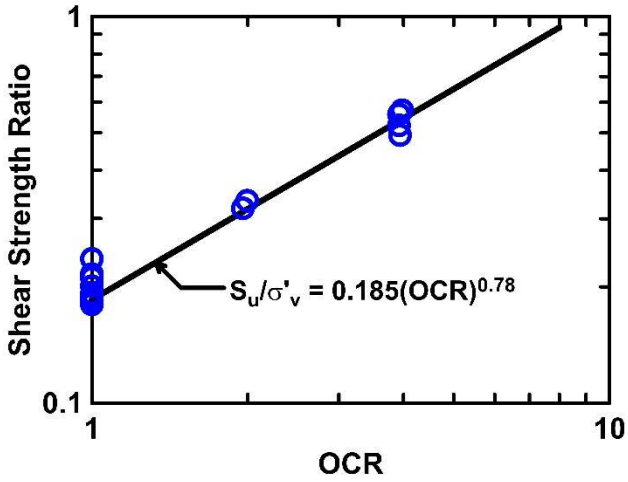

Figure 8: Relationship between undrained shear strength ratio and OCR based on DSS tests performed by Woodward-Clyde (1982)

2.3.2 Interbedded Zone and Stiff Clay General Properties

The interbedded zone consists of overconsolidated BCC with thin lenses of silts and fine sands (Shannon and Wilson 1964). This interbedded layer is modeled as one fine grained layer as it is primarily clay and the cohesionless zones within this layer are not thought to be continuous (Beaty and Dickenson 2015). The stiff clay layer is a silty clay with coarse sand (Shannon and Wilson 1964). The data available for estimating the strength characteristics of these layers are limited and somewhat uncertain compared to the sensitive BCC. This study assumes the strength characteristics of the interbedded and stiff clay layers to be similar as they are both stiff deposits of BCC. The limited data in each layer is used to estimate a common $S_{u,pk}/\sigma'_v$ value for both layers. Idriss (1985) reports the OCR of the interbedded zone to be as high as 4 which corresponds to a $S_{u,pk}/\sigma'_v$ value of 0.55 using equation 1. The OCR for the stiff clay layer may be as low as about 1.3 indicating a $S_{u,pk}/\sigma'_v$ of 0.23 using equation 1. Though this OCR information is limited to a few samples in the upper few meters of the stiff clay deposit (Idriss 1985). CPT data collected near the Fourth Avenue site by Woodward-Clyde (1982) is highly variable in the upper 30 m where

the interbedded zone exists which may be due to the presence of thin dense sand seams. The CPT data becomes more consistent below the sand layer with $S_{u,pk}/\sigma'_v$ values generally centered about 0.20 in the stiff clay using the procedure of Robertson (2009) and a N_{kt} value of 14 (Figure 9). A $S_{u,pk}/\sigma'_v$ value of 0.35 was used in this study for both the interbedded and stiff clay layers. The shear wave velocities for the interbedded and stiff clay layers were estimated to be 300 m/s and 450 m/s respectively.

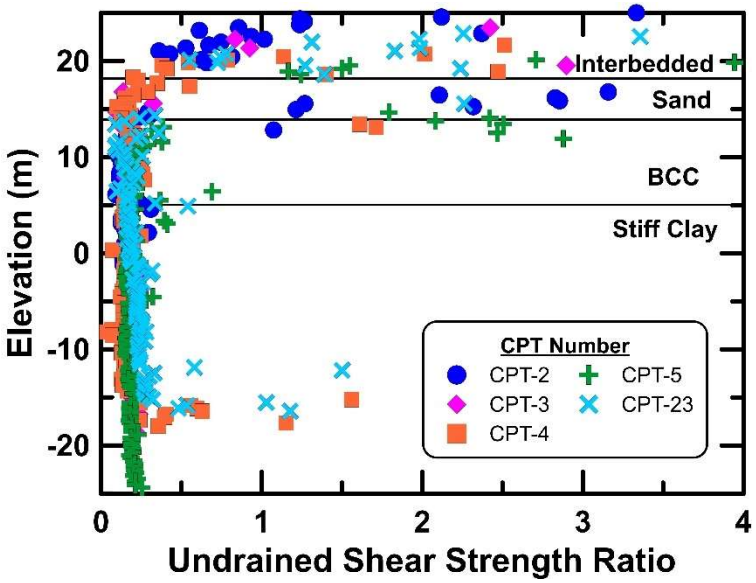

Figure 9: Undrained shear strength ratio estimated from CPTs performed by Woodward-Clyde (1982)

2.3.3 Sand and Outwash General Properties

The outwash deposit consists of dense gravels and sands (Idriss 1985) and the sand layer consists of finer dense silty sands (Shannon and Wilson 1964). The strength characteristics of these coarse-grained soils were estimated from SPTs performed by Shannon and Wilson (1964) in the form of $(N_1)_{60}$ values (Figure 10). The sand and outwash layers were estimated to have average $(N_1)_{60}$ values of about 45 and 50 respectively. This study uses friction angles of 38 and 35 for the sand outwash and sand layers, respectively, which are the values used by Beaty and Dickenson

(2015). It should be noted these friction angle values are slightly lower than would be predicted based on the corresponding $(N_1)_{60}$ values using relationships published by previous researchers (e.g., Teng 1962, Peck et al 1974, Bowles 1996). A shear wave velocity of 300 m/s was estimated for both the sand and outwash layers (Nath et al. 1997).

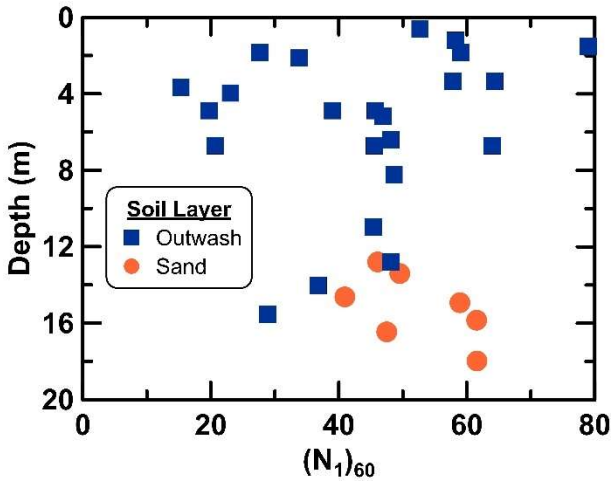

Figure 10: $(N_1)_{60}$ values estimated from SPTs performed by Shannon and Wilson (1964)

2.4 Ground Motions

No ground motion recordings exist from the Great Alaska Earthquake, so recordings from other large magnitude subduction zone quakes were used in this study. All recordings were downloaded from the Center for Engineering Strong Motion Data database (CESMD 2017). Pre-processed recordings from four stations were selected from the 2010 M8.8 Chile earthquake. Raw recordings from two stations were selected from the 2011 M9.0 Tohoku earthquake in Japan and processed according to the guidelines provided by Ancheta et al. (2013). The two horizontal components from each station were considered independently for a total of 12 ground motion records. Selected properties of each motion are shown in Table 2. A target spectrum for the Fourth Avenue site was previously developed by Beaty and Dickenson (2015) using ground motion

prediction equations for subduction zone events (Figure 11). The horizontal components of ground motions were linearly scaled to match this target spectrum between periods of 0.6 to 1.0 seconds, which roughly encompasses the low strain period of the site. Vertical and horizontal components of each motion were used with the same scaling factor applied to each. The spectral accelerations at short periods are higher in the scaled motions than the target spectra (Figure 11), but the range of acceleration values from the scaled records is consistent with results from regional ground motion simulations of this event performed by Mavroeidis et al. (2008). The range of PGAs for the scaled records varies between 0.16g to 0.35g which is consistent with the estimates of Moriwaki et al. (1985) and the simulations performed by Mavroeidis et al. (2008).

Table 2: Properties of selected input motions

Earthquake Name	Station ID	CH	Mw	Epicentral Distance (km)	Scale Factor	PGA of Scaled Motion (g)	Arias Intensity (m/s)	V_{S30} (m/s)
Chile 2/27/2010	CUR	NS	8.8	171	0.60	0.28	3.8	525
		EW			0.55	0.23	3.3	
	HUA	L	8.8	136	0.43	0.16	1.4	530
		T			0.43	0.19	1.6	
	LLO	L	8.8	274	0.50	0.22	1.2	370
		T			0.40	0.16	1.6	
	TAL	L	8.8	113	0.70	0.33	5.6	550
		T			0.60	0.25	3.9	
Japan 3/11/2011	FKS 015	NS	9.0	227	1.25	0.35	2.5	696
		EW			1.0	0.22	1.4	
	TCG 001	EW	9.0	253	0.70	0.20	1.2	580
		EW			0.70	0.29	1.8	

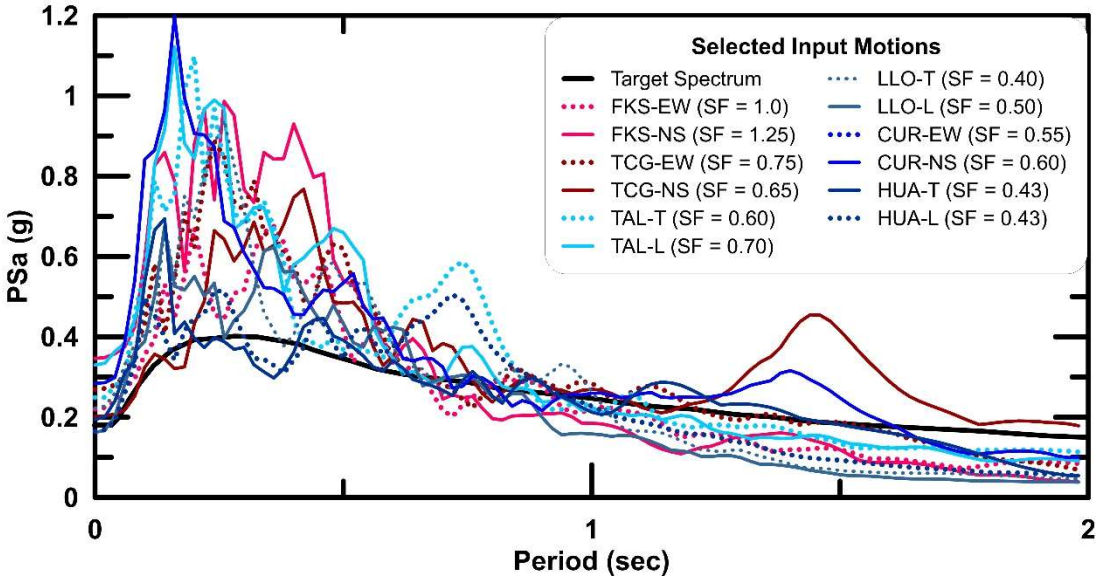

Figure 11: Pseudo-spectral acceleration (PSa) response spectra for scaled motions compared to Fourth Avenue landslide target spectrum developed by Beaty and Dickenson (2015)

CHAPTER 3: REGULARIZED STRAIN SOFTENING MOHR-COULOMB MODEL

Note: The simulations presented in this chapter are based on research previously published in Kiernan and Montgomery (2018). Details of the simulations, including model input parameters, have been changed to be more consistent with the simulations presented in the next chapter. The results obtained were consistent with those of Kiernan and Montgomery (2018). The text and formatting have been modified to fit the organization and style of this thesis.

The purpose of this chapter is to demonstrate the use of a relatively simple strain softening model to examine potential deformations from cyclic softening of sensitive clays. The model uses a Mohr-Coulomb based formulation which has been modified to allow for strain softening. The model requires few input parameters and the issue of mesh dependency after softening is addressed using a softening-scaling regularization approach (Pietruszczak and Mróz 1981). The use of the model is demonstrated through an analysis of the Fourth Avenue slide. A limited numerical sensitivity study is performed to examine the effect of varying the mesh size, the input ground motion and the BCC sensitivity on the results. Potential uses and limitations of this model are discussed.

3.1 Selected Constitutive Model

This chapter uses the total stress Mohr-Coulomb model that incorporates strain softening. The Mohr-Coulomb yield surface is a hexagonal pyramid in principle stress space which makes an equal angle with each principle stress axis. The Mohr-Coulomb yield surface (K_f line) can also be visualized as a function of mean effective stress (p') and deviatoric stress (q) (Figure 12a). The slope and position of the yield surface is defined by the material friction angle (ϕ) and cohesion intercept. Strain softening Mohr-Coulomb models allows the properties of the model to change with increasing plastic strain (Itasca 2016). The yield surfaces at the peak and residual strength

states for a Mohr-Coulomb model with strain softening are shown in Figure 12b with the yield surface now represented by an undrained shear strength with a friction angle of zero.

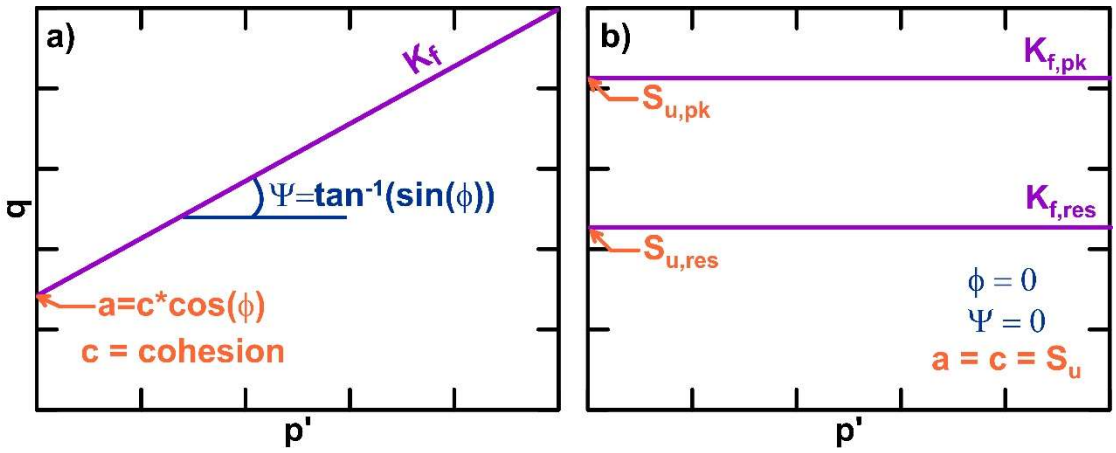

Figure 12: K_f lines for (a) standard Mohr-Coulomb model under drained loading with a given friction angle and cohesion intercept; (b) strain softening Mohr-Coulomb model for undrained loading with friction angle of zero and given values of peak and residual undrained shear strength

Strain softening Mohr-Coulomb models have been used by Potts et al. (1990) to examine the progressive failure of a dam and by Anastasopoulos et al. (2007) to examine fault rupture propagation through sand. The model used in this chapter is a modification of the strain hardening/softening constitutive model implemented in the commercial finite difference software FLAC (Itasca 2016). Further details of the formulation and implementation of the model are discussed in Itasca (2016).

The version of the model used in this study only considers softening of the cohesion with increasing plastic deviatoric strain (Figure 13a). The amount of softening is specified using a clay sensitivity (S_t), which relates the peak undrained shear strength (cohesion) to the remolded undrained shear strength (Figure 13a). The rate of softening is specified using a strain to remold

(γ_{rem}). In the current model, softening is assumed to occur within a thin shear band and the corresponding element behavior is derived using a softening scaling approach as discussed below.

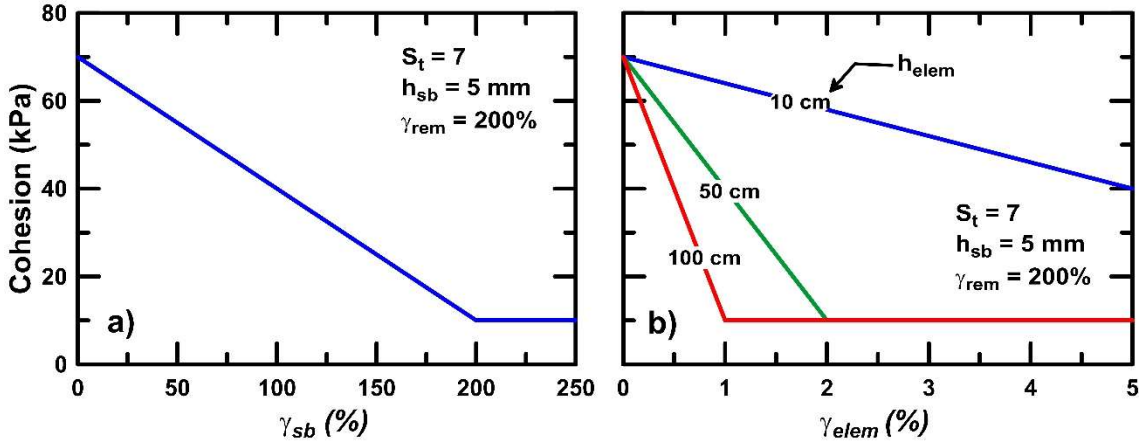

Figure 13: Strain softening in the selected model at (a) the shear band level and (b) the corresponding behavior at the element level after applying softening-scaling

A length scale was implemented into the strain softening Mohr-Coulomb model following the softening-scaling approach proposed by Pietruszczak and Mráz (1981) to reduce the effects of mesh dependency on the solution. This method scales the rate of softening based on the size of the element to keep the ratio of the softening rate and element size constant. The concept of this approach is illustrated in Figure 14. In the current implementation this is done by linearly scaling the plastic deviatoric strain at the element level (γ_{elem}) to approximate the magnitude of strain (γ_{sb}) that would have occurred in a shear band of thickness h_{sb} for the same overall displacement. This scaled strain is then used to calculate an amount of softening and the cohesion for the element is reduced based on the assigned S_t value. This process is demonstrated in Figure 13b. A similar softening-scaling approach has been used successfully by previous researchers to obtain mesh insensitive solutions for localization problems in both sands (e.g., Anastasopoulos et al. 2007) and clays (e.g., Brinkgreve 1994, Andresen and Jostad 1998). One drawback of this approach is that

the thickness of the shear band (h_{sb}) and the rate of softening (γ_{rem}) must be assumed by the user at the start of the simulation. These values are difficult to obtain from standard laboratory tests but can be assumed based on values in literature (e.g., Thakur 2007, Gylland et al. 2014).

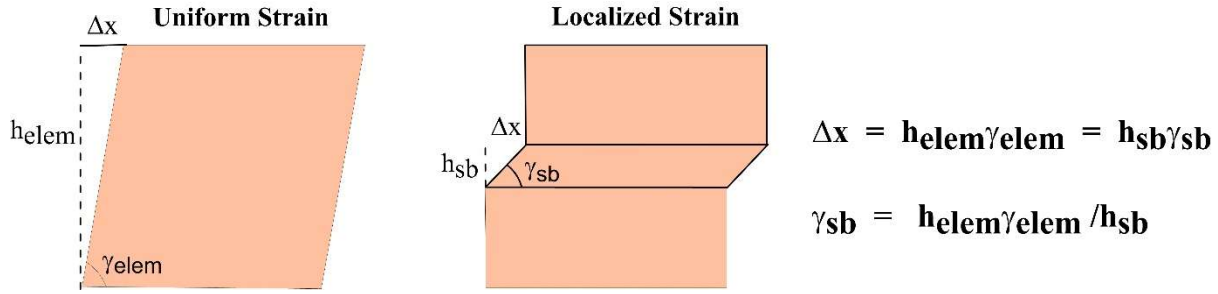

Figure 14: Illustration of softening-scaling approach

3.2 Regularized Strain Softening Model Numerical Simulations

Numerical simulations were performed to examine the ability of the constitutive model discussed above to reproduce the pattern and magnitude of displacements observed at the Fourth Avenue slide. Simulations were performed using FLAC, Version 8.0 (Itasca 2016). The critical BCC layer is modeled using the regularized strain softening model described above, which was implemented as a user defined material in a dynamic link library (DLL). Other layers were modeled using the standard Mohr-Coulomb model implemented in FLAC (Itasca 2016) to isolate the effects of the strain softening model on the overall response. The edges of the model were extended approximately 300 m and 200 m beyond the upper and lower edges of the slope, respectively, to reduce the effects of the boundaries. The baseline mesh (referred to as the coarse mesh) included a total of 6,707 elements and an average element size in the BCC of 1.8m. Numerical sensitivity related to mesh size was examined using finer meshes with average mesh size decreased by factors of 1.5 (15,558 elements; referred to as the medium mesh) and 2 (26,828 elements; referred to as the fine mesh). Numerical sensitivity of the results to the chosen mesh size will be discussed in later sections.

3.2.1 Regularized Strain Softening Model Input Parameters

A BCC S_t value of 7 was used for the baseline simulations as this value was found to produce displacements consistent with site observations. The effect of changing the S_t value on the numerical results will be examined later. Two additional parameters need to be specified for the strain softening model, h_{sb} and γ_{rem}. These parameters are not independent (Figure 13) and using a larger h_{sb} with a correspondingly smaller γ_{rem} will yield the same overall element behavior. For the baseline simulation, h_{sb} was assumed to be equal to 5mm and γ_{rem} = 200%. This value of γ_{rem} is consistent with experimental results (e.g., Gylland et al. 2014), but identical results would have been obtained using h_{sb} = 1mm and γ_{rem} = 1000% or h_{sb} = 1cm and γ_{rem} = 100%.

3.2.2 Regularized Strain Softening Simulation Procedure

The numerical simulations were conducted in two stages. During the first stage, static stresses were initialized by placing one row of elements at a time and solving for static equilibrium using drained strengths. The water table was then raised in stages to its final level (Figure 3). During this stage, the base of the model was fixed while the side boundaries were fixed in the horizontal direction. During the second stage, vertical and horizontal quiet boundaries were used along the base of the model and free-field boundaries were used along the sides to simulate the earthquake shaking. Details of these dynamic boundary conditions are provided by Itasca (2016). The strength properties for all layers were then updated for dynamic loading. The undrained shear strength of the sand and outwash layers were set equal to their respective drained Mohr-Coulomb strengths using the effective stress in each zone after reaching static equilibrium. The fine grained layers were assigned undrained strengths defined in chapter 2. Both the vertical and horizontal components of the selected input motion were applied to the base of the model as stress time

histories. Simulations were run until the end of shaking or until the simulation stopped due to excessive deformation of the mesh. No re-meshing was used in these simulations.

3.3 Simulation Results

A baseline simulation was performed to examine the ability of the modeling approach described above to approximate the displacements observed at the Fourth Avenue landslide. The baseline analysis utilized the HUA-T input motion, the coarsest mesh and a clay sensitivity of 7 for the BCC layer. The softening parameters h_{sb} and γ_{rem} were assumed to be 5 mm and 200%, respectively.

Results from the baseline model show a large translational failure developing in the slope (Figure 15) with peak lateral displacements of the crest of the uppermost slope approaching 4.6m. This value is lower than the observed displacement of 5.3m, but the pattern of displacement is similar to observations (Shannon and Wilson 1964). Displacement of the upper crest is shown along with the input acceleration in Figure 16. Large displacements do not begin to develop until approximately 30 seconds after shaking begins, which corresponds to the start of very strong shaking. At this point the strain in the elements along the base of the BCC reaches the remolding strain and the strength is reduced to its residual value. The slope then continues to move through the end of the record, although the velocity levels off as the shaking intensity reduces.

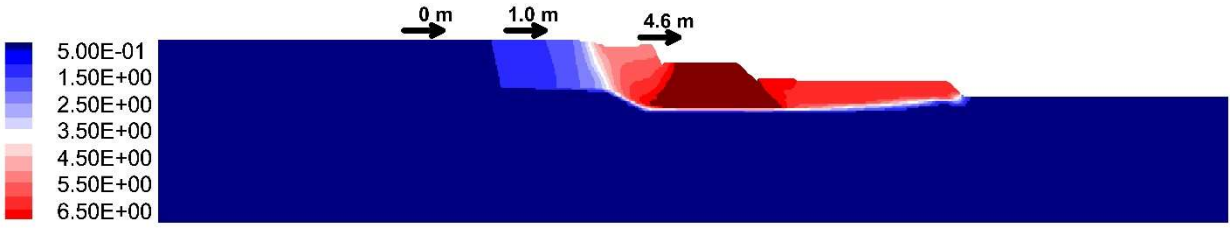

Figure 15: Lateral upper crest displacement contours in meters for baseline regularized strain softening model with HUA-T input motion

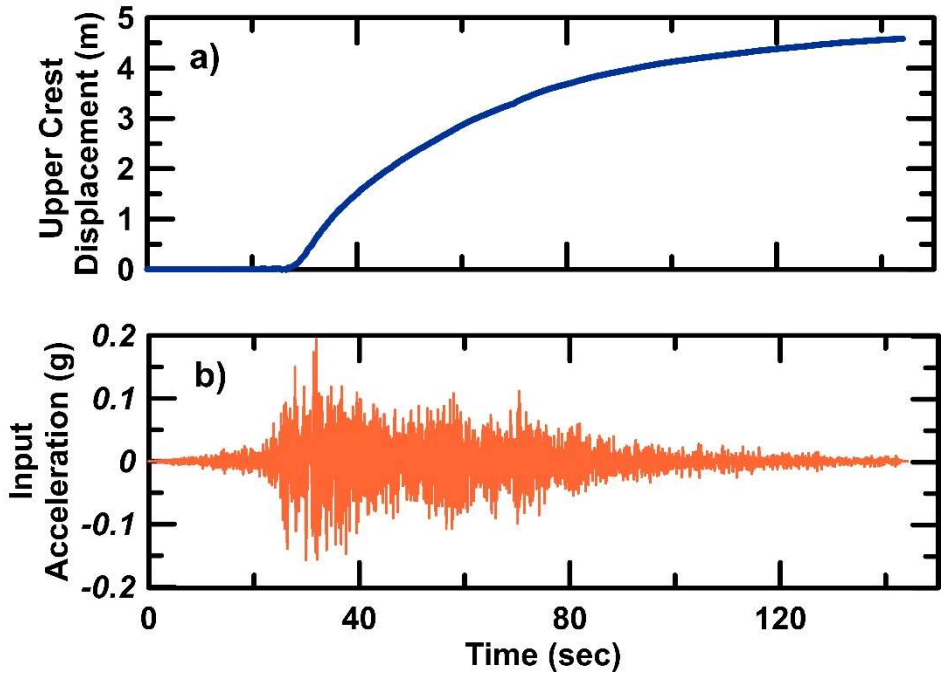

Figure 16: Time histories of (a) upper crest lateral displacement and (b) input acceleration with HUA-T motion for baseline regularized strain softening model

3.3.1 Effects of Input Ground Motion on Regularized Strain Softening Model Simulations

The effect of the input ground motion on the results was examined by repeating the baseline simulation with the 12 ground motions shown in Figure 9. All the simulations show a very similar pattern of lateral displacement although the magnitude of displacement varies. This variation is shown in Figure 17 where the displacement of the upper crest is plotted versus the Arias Intensity of the scaled motion. Arias Intensity has previously been shown to correlate with seismic slope displacement as it combines the effects of intensity and duration (Travasarou et al. 2003). The simulation results show that displacement tends to increase with increasing Arias Intensity. The HUA-T motion gives approximately median displacements and so was used in the remaining simulations.

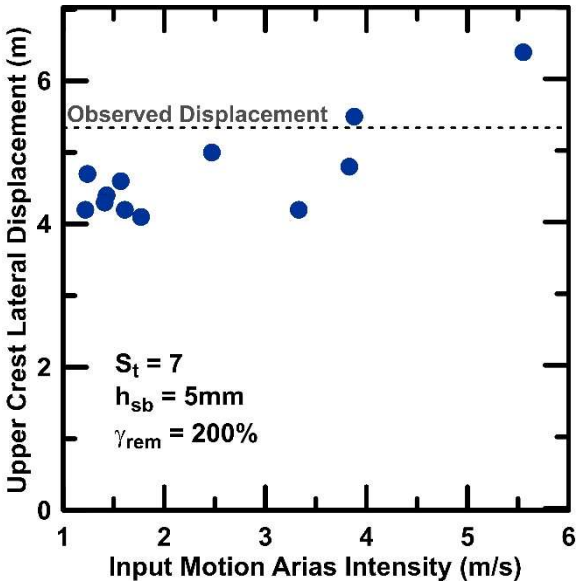

Figure 17: Comparison of upper crest displacement versus Arias Intensity for selected motions using regularized strain softening model

3.3.2 Effect of BCC Sensitivity on Regularized Strain Softening Model Simulations

The influence of S_t for the BCC layer was analyzed by repeating the baseline analyses with the HUA-T motion and S_t values of 3 and 11 which respectively correspond to the mean and maximum BCC S_t values reported by Idriss (1985). The displacements from these two models are compared with the baseline model (S_t = 7) in Figure 18. All three models show that large displacements begin at approximately 30 seconds, which corresponds with the onset of strong shaking (Figure 16b), but the amount of displacement increases with increasing clay sensitivity, as expected. The deformation pattern in all three simulations was similar to Figure 15. The simulations with a S_t value of 11 was stopped before the end of the record due to excessive mesh deformation. The simulation with a S_t of 3 showed relatively little movement as the strength did not drop low enough to cause major instability. These results suggest that using a clay sensitivity between 7 and 11would produce displacements consistent with observations (~5.3m).

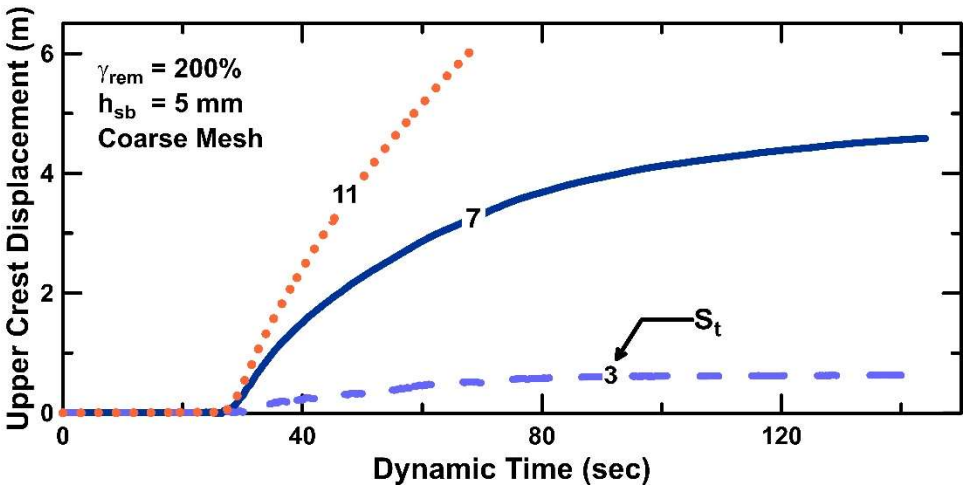

Figure 18: Time histories of upper crest displacement for three BCC sensitivity values using regularized strain softening model

3.3.3 Effect of Mesh Density on Regularized Strain Softening Model Simulations

The ability of the softening scaling to reduce numerical sensitivity related to mesh size was examined by repeating the baseline analyses using the three mesh densities described above. All results showed very similar displacements including a translational failure and nearly identical shear strain contours. Displacements of the upper crest for the three mesh densities are shown in Figure 19a. Onset of large deformations begin at the start of strong shaking and nearly identical rates of displacement are observed up to 4 meters. At this point the mesh becomes too distorted in the finer mesh for the solution to continue. The effect of the softening scaling approach can be demonstrated further by repeating the simulations with the regularization scheme disabled. For these simulations, the softening parameters are specified at the element level rather than the shear band level. γ_{rem} was reduced to 1% to ensure similar element level behavior between the scaled and unscaled simulations for the fine mesh. The results (Figure 19b) show the coarsest mesh experienced only about half the displacement magnitude of the finer two meshes. This occurs because the magnitude of the shear strain in a single element increases with decreasing mesh size

for a given amount of lateral displacement, leading to more softening in finer meshes for the same amount of displacement. The BCC in the finer meshes was therefore able to fully soften during strong shaking while the BCC in the coarse mesh did not. The regularization technique used in this chapter overcomes this by defining the rate of softening at the shear band level and scaling the strain required for softening based on the size of the element.

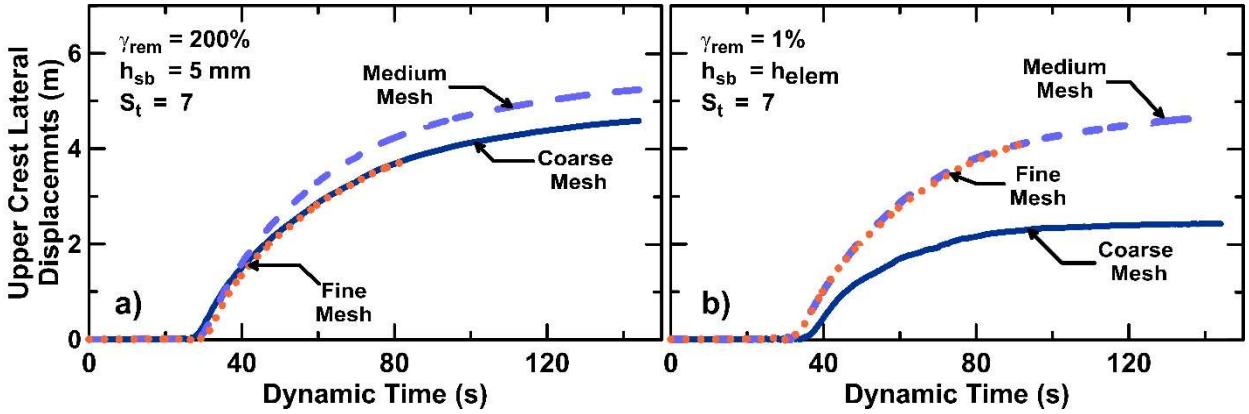

Figure 19: Comparison of upper crest displacement for three mesh densities. Results are shown with the softening-scaling regularization approach (a) and without scaling (b)

3.3.4 Effect of γ_{rem} on Regularized Strain Softening Model Simulations

To investigate the numerical sensitivity of the solution to the selected values for the parameters γ_{rem} and h_{sb}, the baseline analysis was repeated with an increased γ_{rem} (Figure 20). When γ_{rem} is increased to 400%, the response is similar to the baseline model, but large displacements begin slightly later as it takes more strain to reach the same level of softening when γ_{rem} is increased. When γ_{rem} is increased to 600%, not enough strain occurs in the BCC to fully remold the BCC during strong shaking and displacements are limited. Simulations were not performed using smaller values of γ_{rem} but would be expected to lead to faster softening. This demonstrates that the results will be sensitive to the value of γ_{rem} (and correspondingly h_{sb}).

Additional work is needed to further explore this numerical sensitivity and to develop methodologies to reliably estimate these parameters in practice.

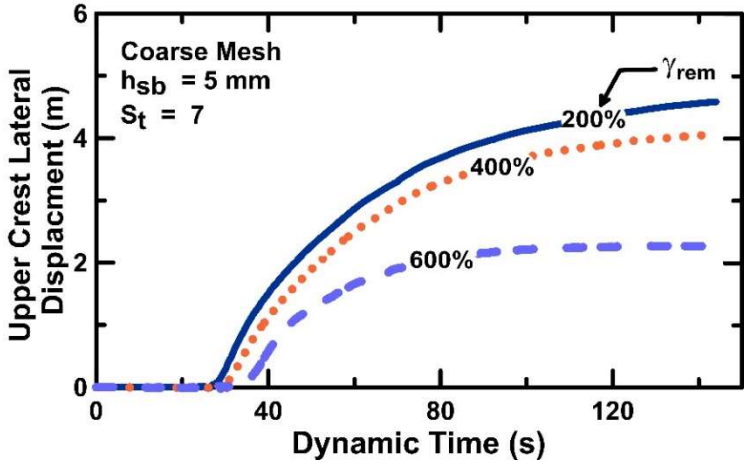

Figure 20: Comparison of upper crest displacement for three remolding strains (γ_{rem}) on the regularized strain softening model simulations

3.4 Discussion and Summary of Regularized Strain Softening Model Simulations

Cyclic softening in clayey soils has led to significant damage to civil infrastructure in previous earthquakes, but methods to model the potential deformations associated with this phenomenon are less developed than those for modeling liquefaction of sandy soils. One complication that may contribute to this is the numerical solution will become mesh dependent after softening occurs and strains localize. There are multiple regularization techniques to overcome this mesh dependency, but many require advanced numerical formulations and effective stress based constitutive models, which may not be publicly available or practical for projects with limited information and resources.

This chapter has demonstrated the ability of a relatively simple strain softening Mohr-Coulomb model to reproduce the pattern of displacements observed for the Fourth Avenue landslide. A length scale was implemented into the model using the softening-scaling approach,

which was shown to give results that were approximately insensitive to mesh size. A limited numerical sensitivity analysis was performed to examine the effect of some of the modeling parameters on the results. Additional analyses are needed to further test the ability of the regularization technique to provide a mesh independent solution, to examine the effects of other parameters on the results and to examine additional case histories. This work is ongoing.

The model and regularization technique require only two extra parameters beyond those needed to define the strength and clay sensitivity of the soil (h_{sb} and γ_{rem}), which were defined in this paper based on values presented in literature. As demonstrated in Figure 13, these values are not independent and identical results will be obtained if the product of the selected values remains constant. Selecting values for specific soils remains a challenge as the thickness of the shear band is not measured in routine lab testing. Advanced numerical simulations (e.g., Thakur et al. 2005) may offer a means to provide reasonable bounds on these parameters.

The model used in this study is a total stress based model that provides a rather crude approximation of the actual dynamic response of a sensitive clay. For example, the model is not able to capture the effects of pore fluid coupling or small strain non-linearity, which may be important for some problems. It also does not consider rate effects, anisotropy or the potential for cracking which was observed at this site. More advanced constitutive models and simulation approaches may be better able to capture these behaviors and additional research in this area is encouraged. Despite these limitations, the proposed modeling approach provides a reasonable approximation for the deformation of the Fourth Avenue landslide and it is hoped that the simplicity of the formulation will make it useful for practicing engineers in the future.

CHAPTER 4: MODIFIED PM4SILT EFFECTIVE STRESS MODEL

Note: The simulations presented in this chapter have been published in Kiernan and Montgomery (2019). The text and formatting have been modified to fit the organization and style of this thesis, but the results are unchanged from this publication.

This chapter uses the recently published PM4Silt constitutive model (Boulanger and Ziotopoulou 2018) to simulate the response of the Fourth Avenue landslide. PM4Silt is a critical state compatible effective stress based bounding surface plasticity model formulated to model the cyclic response of low plasticity fine grained soils. Critical state theory represents a strength limit state of soil in terms of both shear response and volumetric response (Schofield and Wroth 1968). The critical state of a soil is typically defined using equations in p′-q space as well as e-log(p′) space, where e is the void ratio of the soil. The critical state line in e-log(p′) space is shown in Figure 21. The relative locations of the elastic range, critical state line and bounding surface for PM4Silt in p-q space are shown in Figure 22. The bounding surface describes how high the peak undrained shear strength may be compared to the critical state value. Further details on the formulation of PM4Silt can be found in Boulanger and Ziotopoulou (2018).

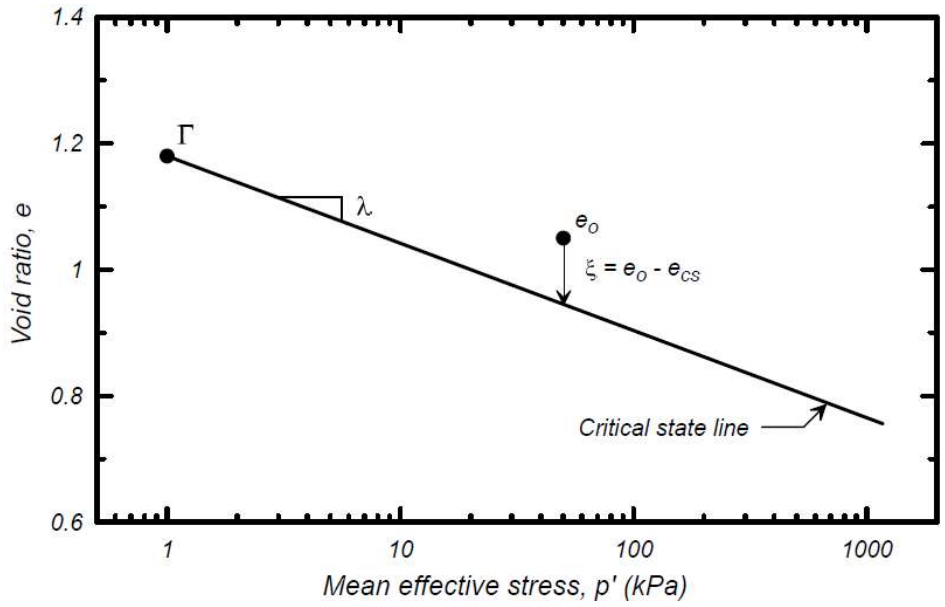

Figure 21: Example of critical state line in e-log(p) space (from Boulanger and Ziotopoulou 2018)

.

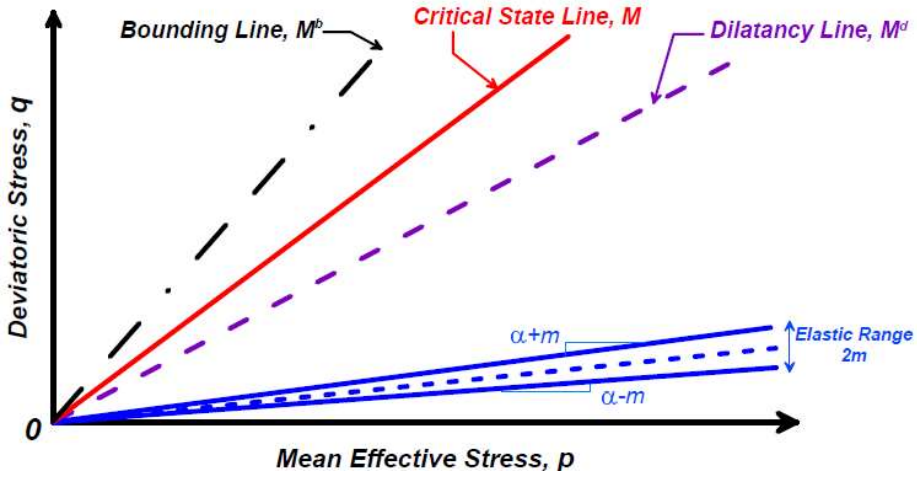

Figure 22: Example of yield, dilatancy, critical state and bounding surfaces for PM4Silt constitutive model (from Boulanger and Ziotopoulou 2018)

This chapter introduces a modification to PM4Silt, which models the response of mildly sensitive clays by accounting for the effects of structural degradation on the critical state line. The modified model is first calibrated using single element simulations and then used to simulate the Fourth Avenue landslide, which failed during the 1964 Great Alaska Earthquake. The influence of the constitutive model parameters on the simulation results is explored. Potential limitations of the proposed approach and possible future improvements are discussed.

4.1 Numerical Simulations Using the Modified PM4Silt Model

The commercial finite difference code FLAC (v8.0, Itasca 2016) was used to perform 2D plane strain simulations. Pre-earthquake stresses were established using a fixed base and roller boundaries along the sides. During this stage, the zones were assigned an elastic, perfectly plastic Mohr-Coulomb constitutive model with stiffness and drained strength parameters described in Chapter 2. Constitutive models are then updated for dynamic loading using the model calibrations described below. During dynamic loading free-field boundaries are applied at the model sides with a compliant boundary along the base. Details on the formulation and implementation of these boundary conditions are given by Itasca (2016).

4.2 Constitutive Models Used for Dynamic Loading in Modified PM4Silt Simulations

In this chapter the non-BCC layers are modeled using the effective stress based PM4Sand and PM4Silt models as described below. These constitutive models are chosen to provide a more accurate system level response as their formulation is able to capture more complex soil behavior including coupling between the soil and pore fluid. It is expected that this more complex formulation will be able to more accurately propagate the seismic energy from the earthquake compared to the elastic-perfectly plastic Mohr-Coulomb formulation used in the last chapter.

The dynamic response of the sand and outwash layers are modeled using PM4Sand Version 3.1 (Boulanger and Ziotopoulou 2017). PM4Sand is a critical state compatible, effective stress-based, bounding surface plasticity model used to model cyclic liquefaction in granular soils. The formulation of PM4Sand is similar to that of the PM4Silt model previously discussed, but PM4Sand uses a critical state line which is curved in e-log(p′) space to represent sand behavior and the default parameters are calibrated to match typical design relationships used in liquefaction analyses (Boulanger and Ziotopoulou 2017). The calibration of PM4Sand was performed using single element direct simple shear simulations and setting the relative density for each layer based on the estimated $(N_1)_{60}$ values using the relationship recommended by Boulanger and Ziotopoulou (2017). The shear modulus coefficients (G_o) were set to achieve the desired shear wave velocities. The h_o parameter was adjusted so that the cyclic modulus reduction behavior for sands matched the curves provided by EPRI (1993) at the appropriate layer depths. The h_{po} parameter was finally adjusted to achieve the desired to cyclic stress ratio (CSR) to cause 3% strain in 15 uniform loading cycles. The target CSR value was calculated using the relationships provided in Idriss and Boulanger (2010) for the estimated $(N_1)_{60}$ values with a cap of 0.8 on the target CSR.

The dynamic response of the stiff clay, interbedded zone and BCC layers were modeled using PM4Silt. PM4Silt utilizes the framework of PM4Sand, but is adapted to better represent the cyclic response of silts and clays as opposed to granular soils. Calibration of PM4Silt was performed using single element direct simple shear simulations with the undrained shear strength at critical state ($S_{u,cs,eq}/\sigma'_v$) set to the estimated values (Table 3). The shear modulus coefficients (G_o) were set to achieve the desired shear wave velocities. The contraction rate parameter (h_{po}) was then adjusted, so that the CSR required to cause 3% shear strain in 30 uniform loadings was equal to 60% of $S_{u,cs,eq}/\sigma'_v$. All calibrations were performed using single element DSS drivers with

σ'_v =100 kPa. Final calibration parameters for the non-BCC layers are summarized in Table 3. Calibration of the BCC layer will be discussed in the next section.

Table 3: Summary of constitutive model input parameters for modified PM4Silt simulations

Layer	$(S_{u,cs,eq}/\sigma'_v)$	$n^{b,wet}$	h_o	h_{po}	G_o	$(N_1)_{60}$
Stiff Clay	0.35	0.8	1.6	2.5	1211	N/A
Interbedded	0.35	0.8	1.7	2	1303	N/A
Sand	N/A	N/A	0.65	0.034	1177	50
Outwash	N/A	N/A	0.62	0.012	2000	45

4.3 Modification of PM4Silt

PM4Silt is a critical state-compatible model, which means that the final undrained strength of the soil is determined by the initial void ratio (e_o) of the clay and the position of the critical state line (CSL) (Boulanger and Ziotopoulou 2017). Within the model, the position of the CSL is set by $S_{u,cs,eq}/\sigma'_v$ and the peak strength is set by adjusting the calibration parameter $n^{b,wet}$. For insensitive clays, this approach works well, but for sensitive clays the difference between the peak and remolded strength may be large and this calibration process becomes difficult. To overcome this, the PM4Silt model was modified to allow the position of the CSL (defined through the intercept Γ) to move during shearing to represent progressive structural degradation of the sensitive BCC toward a residual limit (Figure 23a). This is conceptually similar to the movement of the normal compression line, which has been observed in sensitive clays (e.g., Yong and Nagaraji 1977). In the modified version of the model, the critical state line moves towards the remolded position with increasing plastic shear strain (Figure 23b). The softening process only occurs when the incremental stiffness (i.e., the change in shear stress divided by the change in shear strain) is negative. The modification introduces two additional input parameters. The first is the residual undrained shear strength ratio ($S_{u,res}/\sigma'_v$) which is determined by dividing the peak undrained shear

strength ratio ($S_{u,pk}/\sigma'_v$) by the clay sensitivity (S_t). The second additional input parameter is the remolding strain (γ_{rem}), which controls the interval of strain over which softening occurs.

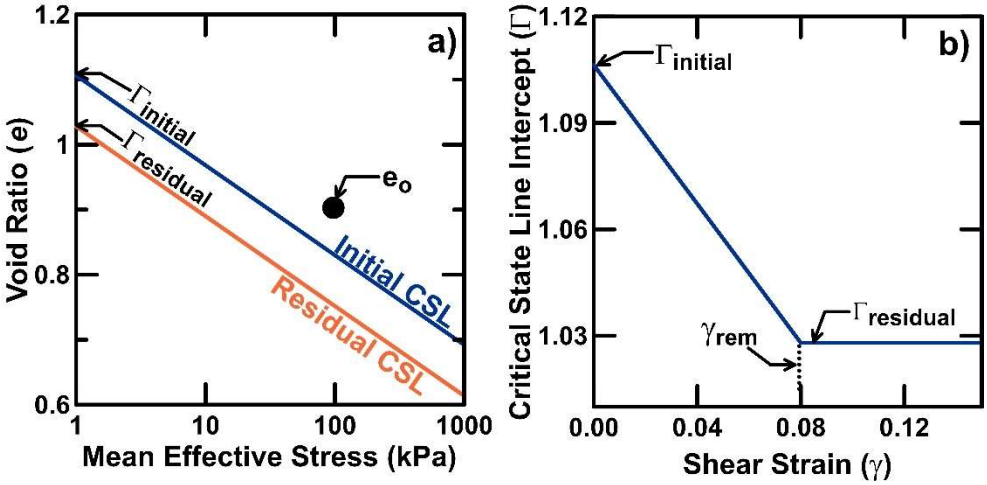

Figure 23: Schematic illustrating the strain softening process in the modified PM4Silt model

The modified PM4Silt model required a slightly revised calibration procedure for the critical BCC layer than described above. All model calibrations were performed using single element DSS drivers with a vertical consolidation stress of 100 kPa as recommended by Boulanger and Ziotopoulou (2017). The parameter G_o was set to 420 to achieve the desired shear wave velocity of 220 m/s. The remolded shear strength is specified through the remolded position of the critical state line (Figure 23). The parameters $n^{b,wet}$ and initial position of the CSL ($\Gamma_{initial}$) are then iteratively adjusted to achieve the desired peak strength using a monotonic DSS driver. The parameter γ_{rem} is then adjusted to change the rate of softening. The parameter h_o was then set to match the modulus reduction curves provided by Vucetic and Dobry (1991) for clays with a PI near 15. The contraction rate parameter (h_{po}) was set last, to achieve the desired cyclic strength (3% strain in 30 cycles with a cyclic stress ratio equal to 50% of the peak undrained shear strength ratio). Final input parameters for all BCC calibrations are shown in Table 4. Figure 24 illustrates

the calibrated model behavior in undrained monotonic and cyclic DSS simulations for a clay sensitivity of 4 and two different rates of softening.

Table 4: Final calibrated BCC input parameters for modified PM4Silt Model

S_t	Softening Rate	$S_{u,res}/\sigma'_v$	$\Gamma_{initial}$	$\Gamma_{residual}$	γ_{rem}	$n^{b,wet}$	h_o	h_{po}
3	Fast	0.075	1.1063	1.0588	0.04	0.65	0.3	17
4	Slow	0.056	1.1063	1.0438	0.08	0.65	0.3	17
*4	Fast	0.056	1.1063	1.0438	0.04	0.65	0.3	17
5	Fast	0.045	1.1063	1.0265	0.04	0.65	0.3	17

*Baseline Calibration

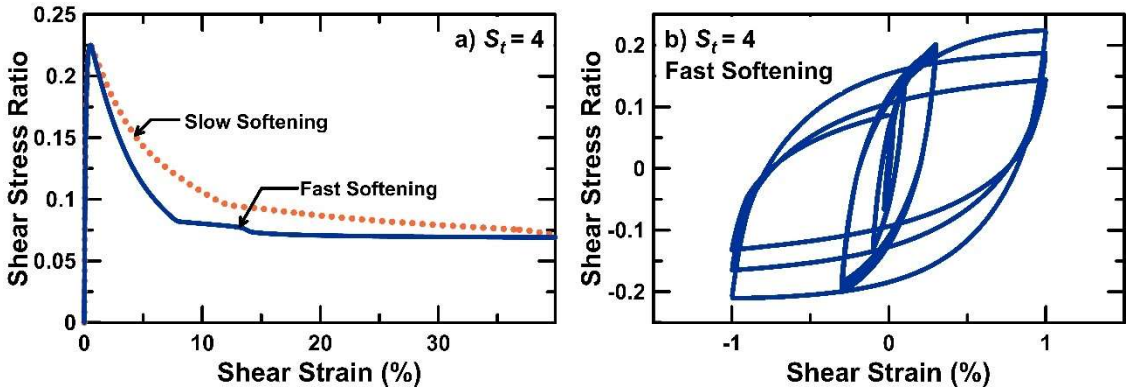

Figure 24: Undrained monotonic (a) and cyclic (b) modified PM4Silt DSS simulation results for a clay sensitivity of 4

4.4 Results and Discussion for Modified PM4Silt Simulations

The baseline simulations for the Fourth Avenue landslide used S_t = 4 and the faster softening rate, along with the HUA-T motion. Lateral displacement contours for the baseline case are shown in Figure 25. Deformation patterns and magnitudes are comparable to those observed at the Fourth Avenue site, including a well-defined translational failure mechanism and a failure plane that intercepts the ground surface just behind the crest of the slope. Shear strains remained roughly horizontal in the BCC until they propagated up to the bluff behind the upper crest. Pressure

ridges can be seen at the toe consistent with observations. The deformation patterns are consistent with the results of Chapter 3 using a strain softening Mohr-Coulomb model, although those models required a higher clay sensitivity value to obtain comparable displacements.

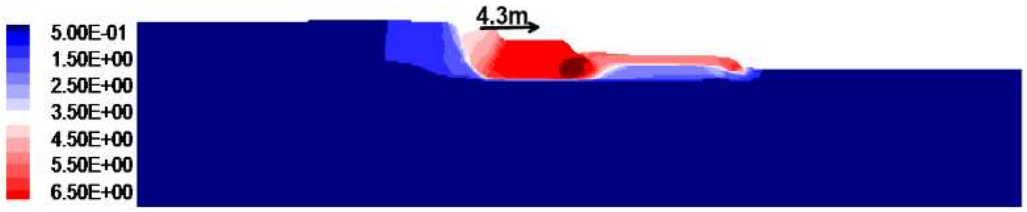

Figure 25: Lateral displacement contours for modified PM4Silt baseline simulation (zero contour omitted)

4.4.1 Effect of Input Motions on Modified PM4Silt Simulations

The effect of input motion was studied by repeating the baseline analyses for the modified PM4Silt simulation with several input motions. Deformation patterns were similar to those shown in Figure 20 across the suite of motions, but deformation magnitudes generally increased with Arias intensity (Figure 26). This increase in displacement with Arias Intensity is consistent with trends shown by previous studies (e.g., Travasarou et al. 2003). A similar trend would likely be observed for other ground motion parameters that incorporate both magnitude and duration, such as the destructiveness potential factor (Araya and Saragoni 1984). The HUA-T motion produces approximately median displacements among the chosen records and is used for the remaining simulations.

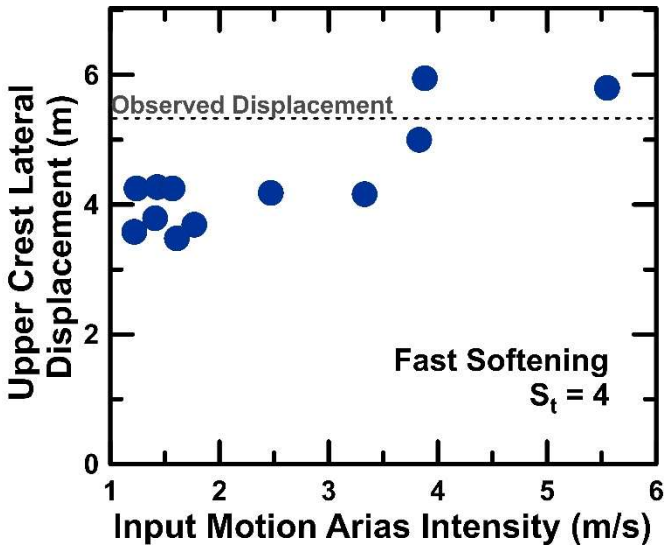

Figure 26: Upper crest displacement versus Arias intensity for selected motions used in modified PM4Silt simulations

4.4.2 Effect of BCC Sensitivity and Softening Rate for Modified PM4Silt Simulations

The effect of the BCC sensitivity was examined by repeating the baseline analysis with a BCC sensitivity of 3 and 5. The effect of increasing the BCC sensitivity on the upper crest lateral displacement is illustrated in Figure 27a. The BCC begins to soften in all three simulations after approximately 35 seconds of shaking, which is where the peak acceleration occurs in the HUA-T motion. The simulation with a BCC sensitivity of 3 showed an upper crest lateral displacement of less than half the observed value. The simulation with a clay sensitivity of 5 was halted before the end of shaking due to excessive mesh deformation. Simulations with the proposed model and a BCC sensitivity between 4 and 5 would likely produce deformations consistent with site observations. This range of clay sensitivities is slightly higher than the mean BCC sensitivities

reported by previous authors (Idriss 1985, Stark and Contreras 1998), but well within the range of measured values.

The effect of the BCC softening rate was examined by repeating the baseline analysis with a softening rate that was approximately half as fast as the baseline simulation (Fig. 27b). The results show that large displacements begin to occur at the same point in the record for both softening rates. The two simulations also reach a similar final displacement value, although the slower softening rate requires significantly more shaking to reach this value. These results indicate that the softening rate does not appear to have a major effect on final deformation magnitudes if the material is able to fully soften during shaking. This is expected as the final deformed shape will be controlled more by the remolded strength (and therefore the clay sensitivity) than the softening rate.

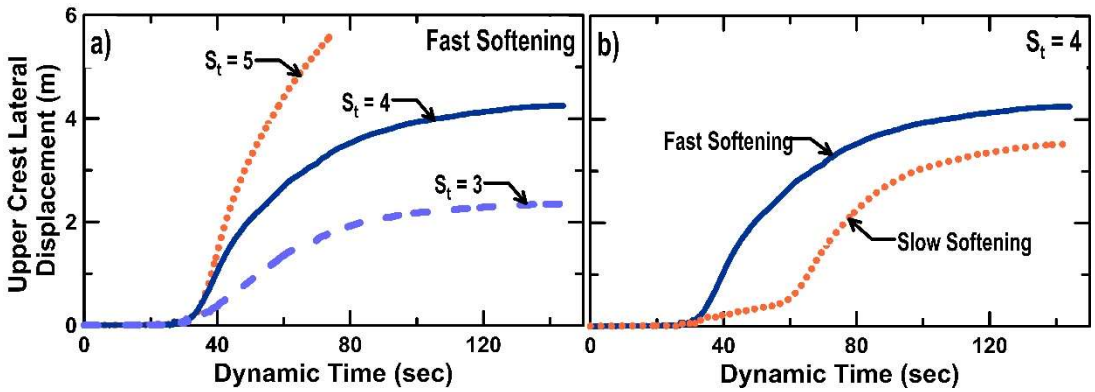

Figure 27: Effect of BCC sensitivity (a) and softening rate (b) on modified PM4Silt simulations

4.4.3 Effect of Mesh Density on Modified PM4Silt Simulations

The effect of mesh density was examined by repeating the baseline analysis with a finer and coarser mesh. All previous analyses utilized a mesh with 14,602 zones with a maximum BCC zone height of 1.3m. A coarser mesh (7,425 zones) and finer mesh (24,298 zones) with maximum

BCC zones heights of 1.8m and 0.9m, respectively, were used to examine the effects of mesh size on the results. The BCC calibration for $S_t = 4$ and the slower softening rate are used in the following simulations to ensure that the fine mesh models are not halted due to geometry errors. Figure 28 illustrates the effect of mesh density on the modified PM4Silt model. All three meshes show displacements beginning to increase after approximately 35 seconds of shaking. The fine mesh shows the fastest increase in displacement after this point, while the coarse mesh only shows a slight increase of displacement with time. The final displacements of the fine and medium meshes are similar although the softening rate is different. This result is expected, as the smaller zones will experience larger strains, and therefore faster softening, for a given magnitude of displacement. These results indicate that the solution is mesh dependent and a regularization scheme to reduce this dependence would be beneficial. The authors are currently implementing a softening-scaling approach similar to the one used in Chapter 3 to address this.

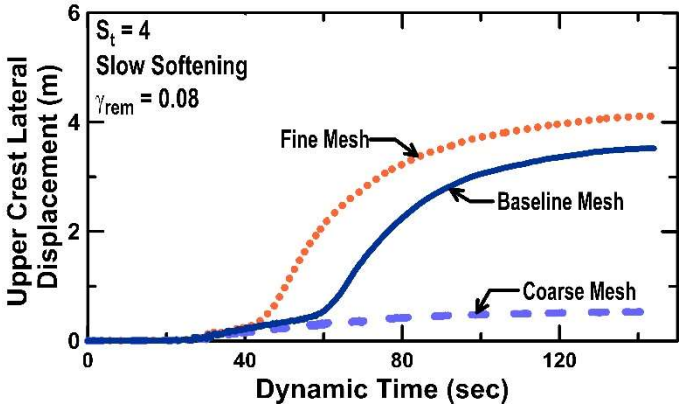

Figure 28: Time histories of upper crest displacement for varying mesh densities

4.4.4 Summary and Conclusions for Modified PM4Silt Simulations

A proposed modification to the existing PM4Silt constitutive model was used to simulate the Fourth Avenue landslide which failed during the 1964 Great Alaska Earthquake. The proposed modification softens the critical state line to a remolded state to replicate structural degradation in

the sensitive BCC. The modification was shown capable of reproducing element level softening behavior in monotonic and cyclic loading in single element DSS drivers. The modification was also shown capable of reproducing system level cyclic softening behavior in full scale simulations of the Fourth Avenue landslide. Deformation patterns and displacement magnitudes observed at the Fourth Avenue site using simulations with the modified PM4Silt model were in reasonable agreement with observations. The softening rate of the BCC did affect the rate of displacement increase but did not significantly affect the final displacement because the duration of loading was sufficient to remold the clay. Mesh dependency of the solution was observed and was most significant for the coarsest mesh, which was not able to fully soften under the imposed loading. Implementation of a regularization technique may be able to address this issue and remains an area for future work. Simulations using additional case histories and lab test are needed to further validate the modified PM4Silt model and identify areas where improvements are needed.

.

CHAPTER 5: SUMMARY AND CONCLUSIONS

This study explored the ability of two separate constitutive models to reproduce deformation patterns and magnitudes observed at the Fourth Avenue landslide which failed due to cyclic softening of a sensitive clay. The first constitutive model studied was a simple total stress Mohr-Coulomb based strain softening model with a softening-scaling based regularization technique employed to reduce mesh dependency of the solution. The second constitutive model studied is the effective stress critical state compatible PM4Silt model which has been modified to represent structural degradation inherent to sensitive clays.

Both models were shown capable of reproducing the deformations observed at the Fourth Avenue site except for the lack of graben formation behind the upper crest. The regularized strain softening model required a BCC sensitivity of 7 to produce deformations comparable to those observed. This clay sensitivity value is much higher than the average value of about 3 reported by previous researchers. Numerical sensitivity studies showed that simulations generally behaved as expected with variations of model input parameters. Deformation magnitudes generally increased with increasing clay sensitivity and decreased as the remolding strain was increased. The BCC sensitivity was found to have a greater effect on the model response compared to the remolding strain. Similar displacements are therefore expected for a given residual strength value if the material fully softens during shaking.

The modified PM4Silt model was able to produce deformations comparable to site observations with a clay sensitivity of 4 which is more consistent with the reported average. The modified PM4Silt simulations utilized material models formulated to represent cyclic softening (i.e., PM4Silt and PM4Sand) in all soil layers, which likely improved the global model response compared to the simple Mohr-Coulomb simulations. Limited numerical sensitivity studies were

also performed for the modified PM4Silt model. Numerical simulations generally behaved as expected with variations of model input parameters. Deformation magnitudes increased with increasing BCC sensitivity and decreased for a slower rate of softening. BCC sensitivity was again found to have a greater effect on deformation magnitudes compared to softening rate. Relatively small variations in BCC sensitivity resulted in significant differences in deformation magnitudes while decreasing the softening rate by a factor of 2 caused only a small decrease in upper crest displacements. This confirms that the residual strength dictates the deformation magnitude if the BCC fully softens during strong shaking.

The softening-scaling approach was found capable of reducing mesh dependency using the regularized Mohr-Coulomb strain softening model. Simulations with the softening scaling regularization enabled resulted in very similar deformation magnitudes across all mesh sizes. The coarse mesh experienced an upper crest lateral displacement with only half the magnitude of the fine and medium mesh when the regularization technique was disabled. This is because the shear strain in the coarse mesh is not large enough to reduce the strength of the BCC to the residual value under the given displacement when the regularization technique is disabled. The softening-scaling approach overcomes this by defining strains based on an assumed shear band thickness rather than the size of the element.

PM4Silt does not currently include a regularization technique and the simulations showed some dependency on the mesh size. Deformation magnitudes of the finer two meshes were comparable as the element sizes were small enough that the given displacements caused the BCC became to fully soften. The coarse mesh experienced minimal displacement as the element sizes and magnitude of imposed loading did not allow for shear strains large enough to reduce the BCC to its residual strength.

Reducing mesh dependency in the modified PM4Silt solution is currently being investigated by the author. One option to reduce mesh dependency of the modified PM4Silt solution is to perform calibrations in terms of displacements rather than strain. For example, once a remolding strain is selected for a given mesh size then the value of displacement required to cause this strain can be used to determine remolding strain values for different zone sizes. This concept is similar to the softening-scaling approach, but strains are scaled to a common displacement value rather than a common shear band thickness. Another option to reduce mesh dependency in the modified PM4Silt model is to use a softening-scaling approach similar to the one used in chapter 3 to scale the element level strains to an assumed shear band thickness. Each of these approaches would likely reduce mesh dependency of the solution. These approaches would not however address the uncertainty involved in selecting the appropriate remolding strain for a given zone size or shear band thickness.

The single case history investigated in this study is not enough to validate each of the proposed constitutive models. Simulations utilizing additional case histories involving cyclic-softening of clay is needed to ensure each model behaves consistently under a variety of situations. Case histories involving monotonic softening of clay are also needed to examine the validity of the proposed models when the loading is not cyclic. Numerical analyses of lab tests involving sensitive clays would further validate each model and could be performed under cyclic and monotonic loading. Evaluation of full-scale case histories with corresponding lab scale simulations would also allow for comparison of appropriate remolding strain and shear band thickness values.

The influence of the non-BCC layers also presents an option for future research. The model input parameters for the non-BCC layers are uncertain due to the lack of characterization data in these layers. Studies to examine the effect of variations in the calibration of the non-BCC layers

would provide insight into how much uncertainty is associated with the input parameters selected for the non-critical layers. The effect of variations in the strength parameters in the non-BCC layers and assumptions regarding drained or undrained loading parameters for the coarse grained layers in the regularized strain softening model should be considered. Variations in the model calibrations for the modified strain softening model should also be evaluated.

Despite the limitations of each model discussed herein it is hoped that they will each be useful for future engineering analyses. The total stress based regularized strain softening model has a straightforward formulation and a relatively simple softening-scaling based regularization that was able to deliver an approximately mesh independent solution. The modified PM4Silt model provides a more realistic representation of stress-strain response and was able to reproduce the observed Fourth Avenue deformation magnitudes using a BCC sensitivity near the mean value reported by Idriss (1985). The modified PM4Silt model exhibited mesh dependence and methods to address this issue are currently under investigation.

REFERENCES

Ancheta et al. (2013). **"**PEER NGA-WEST2 Database." PEER Report 2013/03, Pacific Engineering Research Center, Univ. of California Berkeley

Andresen, L., and Jostad, H. P. (2005). "ANISOFT – Constitutive Model for Undrained Loading of Anisotropic and Strain-Softening Clay." *Geo-Frontiers Congress 2005*, Austin, Texas.

Andresen, L., and Jostad, H. P. (1998). "Effect of strain-softening in interpretation of laboratory compression tests". *Application of Numerical Methods to Geotechnical Problems*, Springer; 223-232.

Anastasopoulos, I., Gazetas, G., Bransby, M. F., Davies, M. C. R., and Nahas, A. E. (2007). "Fault Rupture Propagation through Sand: Finite-Element Analysis and Validation through Centrifuge Experiments." *J. of Geotech. and Geoenviro. Eng*., 133(8), 943–958.

Araya, R. and Saragoni, G.R. (1984). "Earthquake Accelerogram Destructiveness Potential Factor." *Proc. 8th World Conference on Earthquake Engineering 1984*. San Francisco, CA

Beaty, M. H. and Byrne, P. M. (2011). "UBCSAND constitutive model: Version 904aR." Documentation report on Itasca UDM Web Site, February 2011

Beaty, M. H. and Dickenson, S. E. (2015). "Numerical Analysis for Seismically-Induced Deformations in Strain-Softening Plastic Soils." *6th Intern. Conference on Earthquake Geotechnical Engineering*, Chirstchurch, NZ.

Boulanger, R. W., and Ziotopoulou, K. (2017). "PM4Sand (version 3.1): A sand plasticity model for earthquake engineering applications." Report No. UCD/CGM-17/01, Center for Geotechnical Modeling, Department of Civil and Environmental Engineering, University of California, Davis, CA, March, 112 pp.

Boulanger, R. W., and Ziotopoulou, K. (2018). “PM4Silt (Version 1): A silt plasticity model for earthquake engineering applications.” Report No. UCD/CGM-18/01, Center for Geotechnical Modeling, Department of Civil and Environmental Engineering, University of California, Davis, CA.

Bowles, J.E. (1996). *Foundation Analysis and Design*, 5th edn. Singapore, McGraw-Hill.

Brinkgreve, R. B. J. (1994). “Geomaterial models and numerical analysis of softening.” thesis. University of Delft

Center for Eng. Strong Motion Data (CESMD) (2017). http://www.strongmotioncenter.org/

EPRI (1993). Electric Power Research Institute. "Guidelines for determining design basis ground motions." Palo Alto, Calif: Electric Power Research Institute, vol. 1-4, EPRI TR102293.

Elgamal, A., Yang, Z., and Parra, E. (2002). “Computational modeling of cyclic mobility and post-liquefaction site response”. *Soil Dynamics and Earthquake Eng.*, 22(4), 259-271.

Gylland, A. S., Jostad, H. P., and Nordal, S. (2014). “Experimental study of strain localization in sensitive clays.” *Acta Geotechnica*, *9*(2), 227-240.

Gregersen, O. (1981): “The Quick Clay Landslide in Rissa, Norway; The sliding Process and Discussion of Failure Modes.” *International Conference on Soil Mechanics and Foundation Engineering,* 10. Stockholm 1981. Proceedings, Vol. 3, pp. 421-426. Also publ. in: Norwegian Geotechnical Institute. Publication, 135.

Hanson, W. (1965). “Effects of the Earthquake of March 27, 1964, at Anchorage Alaska”. Effects of the Earthquake of March 27, 1964, at Anchorage. USGS Prof. Paper 542-A

Henkel, D. and Skempton, A. (1955). “A Landslide at Jackfield, Shropshire, in a Heavily Over-Consolidated Clay.” *Géotechnique*, 5(2), pp.131-137.

Heritage, R. J. (2013). “Cyclic softening case study: Wendover Retirement Village”. *Proc. 19th NZGS Geotechnical Symposium*. Christchurch , Queensland.

Hsieh, P. G., Ou, C. Y. and Lim, A. (2010). “Use of the total stress undrained model to the analysis of deep excavation.” *Proc. 17th Southeast Asian Geotechnical Conference*, Taipei, Taiwan.

Ichinose, G., Somerville, P., Thio, H. K., Graves, R., and Oconnell, D. (2007). “Rupture process of the 1964 Prince William Sound, Alaska, earthquake from the combined inversion of seismic, tsunami, and geodetic data.” *Journal of Geophysical Research*, 112(B7)

Idriss, I.M. (1985). “Evaluating Seismic Risk in Engineering Practice”. *Proc. 11th Int. Conf. on Soil Mech. and Found. Eng.*, San Francisco, CA. 255-320.

Idriss, I. M. and Boulanger, R. W. (2010). “SPT-based liquefaction triggering procedures.” Report UCD/CGM-10/02, Department of Civil and Environmental Engineering, University of California,

Davis, CA, 259 pp.

Itasca. (2016). FLAC, “Fast Lagrangian Analysis of Continua”, Version 8.0. Itasca Consulting Group, Minneapolis, MN, 2017.

Jostad, H. P., and Andresen, L. (2004). “Modeling of shear band propagation in clays using interface elements with finite thickness”. *Proc. Int. Symp. on Numerical Models in Geomechanics*, Vol. 9, 121-128.

Kiernan, M., and Montgomery, J. (2018). “Numerical Simulations of the Fourth Avenue Landslide Considering Strain Softening.” *Geotechnical Earthquake Engineering and Soil Dynamics V*, Austin, TX, June 10-13th, 2018.

Kiernan, M., and Montgomery, J. (2019). “Modeling the cyclic softening of a mildly sensitive clay.” *7th International Conference on Earthquake Geotechnical Engineering*.”, Rome, Italy.

Lim, A., Ou, C. Y., and Hsieh, P. G (2010). “Evaluation of clay constitutive models for analysis of deep excavation under undrained condition.” *Journal of GeoEngineering,* Vol. 5, No. 1, pp. 9-20.

Locat, A., Locat, P., Demers, D., Leroueil, S., Robitaille, D., and Lefebvre, G. (2017). “The Saint-Jude landslide of 10 May 2010, Quebec, Canada: Investigation and characterization of the landslide and its failure mechanism.” *Canadian Geotechnical Journal*, 54(10), 1357–1374.

Mavroeidis,G.P., Zhang,B., Dong,G., Papageorgiou,A.S., Dutta,U.,and Biswas, N.N. (2008). “Estimation of strong ground motion from the Great 1964 Mw9:2 Prince William Sound, Alaska earthquake.” *Bull. Seismol. Soc. Am*., 98(5), 2303–2324.

Moriwaki, Y., Vicente,E.E., Lai, S. S., Moses, T. L. (1985), "A Reevaluation of the 1964 "L" Street Slide”, Final Report, State of Alaska, Department of Transportation and Public Facilities

Nakamura, S., Wakai, A., Umemura, J., Sugimoto, H., and Takeshi, T. (2014). “Earthquake induced landslides: Distribution, motion and mechanisms.” *Soils and Foundations*, 54(4), 544–559.

Nath, S. K., Chatterjee, D., Biswas, N. N., Dravinski, M., Cole, D. A., Papageorgiou, A., Rodriguez, J. A., and Poran, C. J. (1997). “Correlation Study of Shear Wave Velocity in Near Surface Geological Formations in Anchorage, Alaska.” *Earthquake Spectra*, 13(1), 55–75.

Park, D. S. (2011). "Strength Loss and Softening of Sensitive Clay Slopes." Doctoral Dissertation. University of California, Davis.

Peck, R. B., Hanson, W. E., and Thornbum, T. H. (1974). *Foundation engineering.* John Wiley and Sons, Inc., New York, N.Y.

Pietruszczak, S. and Mróz, Z. (1981). "Finite element analysis of deformation of strain-softening materials*". Int. Jour. for Numerical Methods in Engineering*, 17(3), 327-334.

Potts, D., Dounias, G.,Vaughan, P. (1990). "Finite element analysis of progressive failure of Carsington embankment". *Géotechnique,* 40(1), 79-101.

Robertson, P.K., 2009. "CPT interpretation – a unified approach." *Canadian Geotechnical Journal*, 46: 1-19

Schofield, A. N., and Wroth, P. (1968). *Critical state soil mechanics*. McGraw-Hill, New York.

Shannon and Wilson (1964). "Report on Anchorage area soil studies." Rep. to USACE District, Anchorage, Alaska. Contract no. DA-95-507-CIVENG-64-18.

Seidalinov, G., and Taiebat, M. (2013). "Bounding surface SANICLAY plasticity model for cyclic clay behavior." *Int. J. Numer. Anal. Meth. Geomech.* 38(7), 702–724.

Septanika E, Thakur V, Brinkgreve RBJ, Nordal S (2007) "Modelling undrained instability in geomaterial using extended finite element method (PUM/XFEM)". *Proc. Int. Geomech. Conf.*, Nessebar, Bulgeria

Shield R.T. (1955). "On Coulomb's law of failure in soils." *J. Mech. Phys. Sol.,* 4:10–16

Stark, T. D., Contreras, I. A. (1998). "Fourth Avenue Landslide during 1964 Alaskan Earthquake." *J. of Geotech. and Geoenviron. Eng.,* 124(2), 99–109.

Taiebat, M., Kaynia, A. M., and Dafalias, Y. F. (2011). “Application of an Anisotropic Constitutive Model for Structured Clay to Seismic Slope Stability.” *Journal of Geotechnical and Geoenvironmental Engineering*, 137(5), 492–504.

Teng, W. C. (1962). *Foundation Design*. Prentice-Hall, Inc., Englewood Cliffs, N

Thakur V, Nordal S, Jostad H P, Andresen L, (2005) “Study on pore water pressure dissipation during shear banding in sensitive clays.*” 11th Int. conf. on computer methods and advances in geomech*., G Barla and M Barla Eds, Vol. 4, 289-296

Thakur V, Grimstad G, Nordal S. (2006). “Instability in sensitive soft clays.” *ECI: Geohazards and Risk Evaluation conference*, Farrokh Nadim, Rudolf Pöttler, Herbert Einstein, Herbert Klapperich, and Steven Kramer Eds, ECI Symposium Series, Norway, Vol. P7, http://services.bepress.com/eci/geohazards/43.

Thakur, V. (2007). “Strain localization in soft sensitive clays.” dissertation, Norwegian Centre of Excellence: International Centre for Geohazards.

Travasarou, T., Bray, J. and Abrahamson, N. (2003). “Empirical attenuation relationship for Arias Intensity.” *Earthquake Engineering and Structural Dynamics*, 32(7),1133-1155.

Vucetic, M., and Dobry, R. (1991). "Effect of soil plasticity on cyclic response." *J. Geotech. Engrg.*, 117(1), 89–107.

Woodward-Clyde Consultants (1982). "Anchorage Office Complex, Geotechnical Investigation, Anchorage, Alaska." Rep. to Alaska DOT. and Public Facilities, Design and Constr., Anchorage, Alaska.

Yong, R.N. and Nagaraj, T.S. (1977). “Investigation of fabric and compressibility of a sensitive clay.” *Proc. of the International Symposium on Soft Clay*, Asian Institute of Technology, pp. 327–333.